



U.S. DEPARTMENT OF  
**ENERGY**

Prepared for the U.S. Department of Energy  
under Contract DE-AC05-76RL01830

# Maui Smart Grid Demonstration Project: System Impact Study

KP Schneider  
CA Bonebrake  
AR Fisher  
JL Hammerstrom

October 2012



**Pacific Northwest**  
NATIONAL LABORATORY

## DISCLAIMER

This report was prepared as an account of work sponsored by an agency of the United States Government. Neither the United States Government nor any agency thereof, nor Battelle Memorial Institute, nor any of their employees, makes **any warranty, express or implied, or assumes any legal liability or responsibility for the accuracy, completeness, or usefulness of any information, apparatus, product, or process disclosed, or represents that its use would not infringe privately owned rights.** Reference herein to any specific commercial product, process, or service by trade name, trademark, manufacturer, or otherwise does not necessarily constitute or imply its endorsement, recommendation, or favoring by the United States Government or any agency thereof, or Battelle Memorial Institute. The views and opinions of authors expressed herein do not necessarily state or reflect those of the United States Government or any agency thereof.

PACIFIC NORTHWEST NATIONAL LABORATORY  
*operated by*  
BATTELLE  
*for the*  
UNITED STATES DEPARTMENT OF ENERGY  
*under Contract DE-AC05-76RL01830*

**Printed in the United States of America**

**Available to DOE and DOE contractors from the Office of Scientific  
and Technical Information,  
P.O. Box 62, Oak Ridge, TN 37831-0062; ph: (865) 576-8401 fax: (865)  
576-5728 email: reports@adonis.osti.gov**

**Available to the public from the National Technical Information  
Service,  
U.S. Department of Commerce, 5285 Port Royal Rd., Springfield, VA  
22161  
ph: (800) 553-6847 fax: (703) 605-6900  
email: orders@ntis.fedworld.gov online ordering:  
<http://www.ntis.gov/ordering.htm>**



This document was printed on recycled paper.

(10/2012)

## Table of Contents

TABLE OF FIGURE .....	IV
TABLE OF TABLES .....	V
1 INTRODUCTION .....	1
2 FEEDER BASE CASE CHARACTERISTICS .....	3
2.1 BASE CASE POWER PROFILES .....	6
2.2 BASE CASE VOLTAGE PROFILES .....	8
2.3 BASE CASE TIME-SERIES EXAMINATION .....	10
2.4 BASE CASE CONCLUDING COMMENTS .....	12
3 SOLAR PV ANALYSIS .....	13
3.1 50% PV CASE VOLTAGE PROFILES .....	13
3.2 50% PV CASE VOLTAGE PROFILES .....	15
3.3 50% PV CASE TIME-SERIES EXAMINATION .....	16
3.4 50% PV CASE WITH CLOUD TRANSIENT .....	18
3.5 PV CONCLUDING COMMENTS .....	20
4 EV ANALYSIS .....	21
4.1 INDIVIDUAL TRANSFORMER IMPACTS .....	21
4.2 DISTRIBUTION FEEDER IMPACTS .....	24
4.3 EV CONCLUDING COMMENTS .....	27
5 MICRO DMS ANALYSIS .....	28
5.1 HVAC LOAD SHEDDING DURING SOLAR TRANSIENT .....	28
5.2 PV 4-QUADRANT CONTROL DURING SOLAR TRANSIENT .....	30
5.3 LOAD SHEDDING TO REDUCE EV PEAK .....	32
5.4 BATTERY OPERATIONS TO REDUCE EV PEAK .....	33
5.5 MICRO DMS CONCLUDING COMMENTS .....	35
6 SYSTEM IMPACT STUDY CONCLUDING COMMENTS .....	37
APPENDIX A: GRIDLAB-D SIMULATION METHODOLOGY .....	39
REFERENCES .....	41

## Table of Figure

Figure 2.1: Kihei feeder 1515 .....	4
Figure 2.2: Kihei feeder 1254 .....	5
Figure 2.3: Kihei feeder 1384 .....	6
Figure 2.4: Feeder 1515, base case, transformer and PV power .....	7
Figure 2.5: Feeder 1254, base case, transformer and PV power .....	7
Figure 2.6: Feeder 1384, base case, transformer and PV power .....	8
Figure 2.7: Feeder 1515, base case, voltage profile .....	9
Figure 2.8: Feeder 1254, base case, voltage profile .....	9
Figure 2.9: Feeder 1384, base case, voltage profile .....	10
Figure 2.10: Feeder 1515, base case, time-series for node 32561 voltage .....	10
Figure 2.11: Feeder 1254, base case, time-series for node 31596 voltage .....	11
Figure 2.12: Feeder 1384, base case, time-series for node 23852 voltage .....	11
Figure 3.1: Feeder 1515, 50% PV case, transformer and PV power .....	13
Figure 3.2: Feeder 1254, 50% PV case, transformer and PV power .....	14
Figure 3.3: Feeder 1384, 50% PV case, transformer and PV power .....	14
Figure 3.4: Feeder 1515, 50% PV case, voltage profile .....	15
Figure 3.5: Feeder 1254, 50% PV case, voltage profile .....	15
Figure 3.6: Feeder 1384, 50% PV case, voltage profile .....	16
Figure 3.7: Feeder 1515, difference of base case and 50% PV case, time-series voltage at node N32561 .....	16
Figure 3.8: Feeder 1254, difference of base case and 50% PV case , time-series voltage at node N31596 .....	17
Figure 3.9: Feeder 1384, difference of base case and 50% PV case, time-series voltage at node N32239 .....	17
Figure 3.10: Feeder 1515, comparison of base case and 50% PV case, power factors .....	18
Figure 3.11: Feeder 1515, base case with 1-minute cloud transient, voltage at node N32561 .....	19
Figure 3.12: Feeder 1515, difference of base case with and without 1-minute cloud transient, voltage difference at node N32561 .....	19
Figure 3.13: Feeder 1515, 50% PV case with 1-minute cloud transient, voltage at node N32561 .....	19
Figure 3.14: Feeder 1515, difference of 50% PV case with and without 1-minute cloud transient, voltage difference at node N32561 .....	20
Figure A.1: GridLAB-D architecture .....	39
Figure A.2: Variable step sizes in GridLAB-D simulation .....	40

## Table of Tables

Table 2.1: Kihei Feeder Characteristics .....	3
---	---

# 1 Introduction

The rapid growth of renewable resources on the Hawaiian Islands, in the form of distributed solar PV and central wind, has begun to cause operational issues for the Hawaiian Electric Company (HECO), and subsidiary companies such as the Maui Electric Company (MECO). The island of Maui is an example of a small island system with a high penetration of renewable resources. Maui has a peak load of approximately 200MW with fossil generation resources of 260MW, 72 MW of wind generation scheduled to be online by the end of 2012, and 19 MW of distributed solar PV. The deployment of renewable generation is being driven by two factors. The first is the islands dependence on fossil fuels that have to be shipped to the island, and the second is the State of Hawaii's RPS requirement that requires 40% of generation be provided by renewable resources by 2030.

In an attempt to address the issues that will arise due to the high levels of renewable resources, the Japan U.S. Island Grid Project, formerly the Maui Smart Grid Demonstration Project, will examine the impacts of high penetrations of PV, and develop new operational control strategies to enable higher penetration levels of renewable resources. Specifically, the Japan U.S. Island Grid Project is examining the use of Distribution Management Systems (DMS), microDMS, an Electric Vehicle (EV) control center, smart inverters, community Battery Energy Storage Systems (BESS), and EV-BESS to enable higher penetration levels.

The role of the Pacific Northwest National Laboratory (PNNL) in this project is to perform a System Impact Study (SIS) to examine the impacts of high penetrations of renewable generation, and to examine possible mitigation strategies. The SIS will be divided into three sections. The first two sections will examine new technologies and their impacts, and the third section will examine possible mitigation strategies.

In the first section of the SIS, the effects of distributed solar PV are examined, with a focus on the impact to line voltages. Both the voltage profile of the feeder and the time-series voltage of a specific node are examined. The voltage profile for the current penetration levels of solar PV, as of February 19<sup>th</sup>, and for a hypothetical 50% penetration level is examined. The time-series voltages of a single node over a 24-hour period are examined to see how the diurnal cycle of end-use loads affects voltage. Next, higher resolution time-series simulations are performed to examine the impact of cloud transients, both with the current penetration levels of PV, and with a hypothetical 50% penetration level. A simple but aggressive cloud passing is used to determine the near worst case scenario.

EVs, when deployed in relatively large numbers at the distribution level, have the capacity to address the intermittency of transmission level wind generation. The second section of the SIS

examines the impacts of EV to transformer loading, both at the service and substation level. Similar to the PV study, time-series simulations over a 24-hour period will be examined to see how the diurnal cycle affects voltage.

The third section of the SIS examines the ability of microDMS to mitigate issues presented in the first two sections. Four specific microDMS functions are examined:

- 1) load shedding to mitigate solar induced voltage transients
- 2) 4-quadrant inverters to mitigate solar induced voltage transients
- 3) load shedding to mitigate transformer overloading due to EV charging
- 4) batteries to mitigate transformer overloading due to EV charging

The simulation and analysis performed for the SIS will be conducted in the GridLAB-D simulation environment. Appendix A is provided as a reference for this simulation and analysis tool.

## 2 Feeder Base Case Characteristics

For the SIS, three 12.47 kV distribution feeders from the Kihei substation on the island of Maui, are examined; feeders 1515, 1254, and 1384. These feeders were selected by HECO and MECO as being representative of those that were part of the Japan U.S. Island Grid Project. The key characteristics of these feeders are shown in Table 2.1. These were the characteristics of the feeders as of February 2012, and will be considered the “base case” conditions.

From Table 2.1, it can be seen that the three feeders already have a sizable penetration of distributed solar PV. The breakdown of percent residential (R), percent commercial (C), and percent industrial (I) for each feeder is given. Table 2.1 includes the known installations as of February of 2012. For the simulations presented in this report, the climate values that drove the behavior of the PV were obtained from sensors deployed by the National Renewable Energy Laboratory (NREL). Since specific information for each of the solar panels and their associated inverters was not available, industry standard values were assumed for all units. These include standard unit sizes, and typical inefficiencies due to dirty solar panels and inverter losses.

Table 2.1: Kihei Feeder Characteristics

Feeder	Peak Load (kW)	PV (%)	R (%)	C (%)	I (%)
1515	6,246	9.7%	95.5%	4.5%	0.0%
1254	2,669	12.2%	5.1%	94.9%	0.0%
1384	1,659	18.6%	54.8%	45.2%	0.0%

Figure 2.1, Figure 2.2, and Figure 2.3 show the diagrams of feeders 1515, 1254, and 1384 respectively. A select number of nodes are labeled for later reference in the SIS, including the substation Load Tap Changers (SS-LTC). From these figures and Table 2.1, it can be seen that feeder 1515 is a relatively large and complex residential feeder with a peak load of approximately 6,200 kW. Feeder 1254 is a moderately sized commercial feeder with a peak load of approximately 2,600 kW. Feeder 1384 is a small feeder, composed of a large percentage of overhead 336 AA conductors, with an even mix of residential and commercial loads; peak load is approximately 1,600 kW. The different feeder characteristics and different load compositions provide a representative cross-section of the MECO feeders behavior.



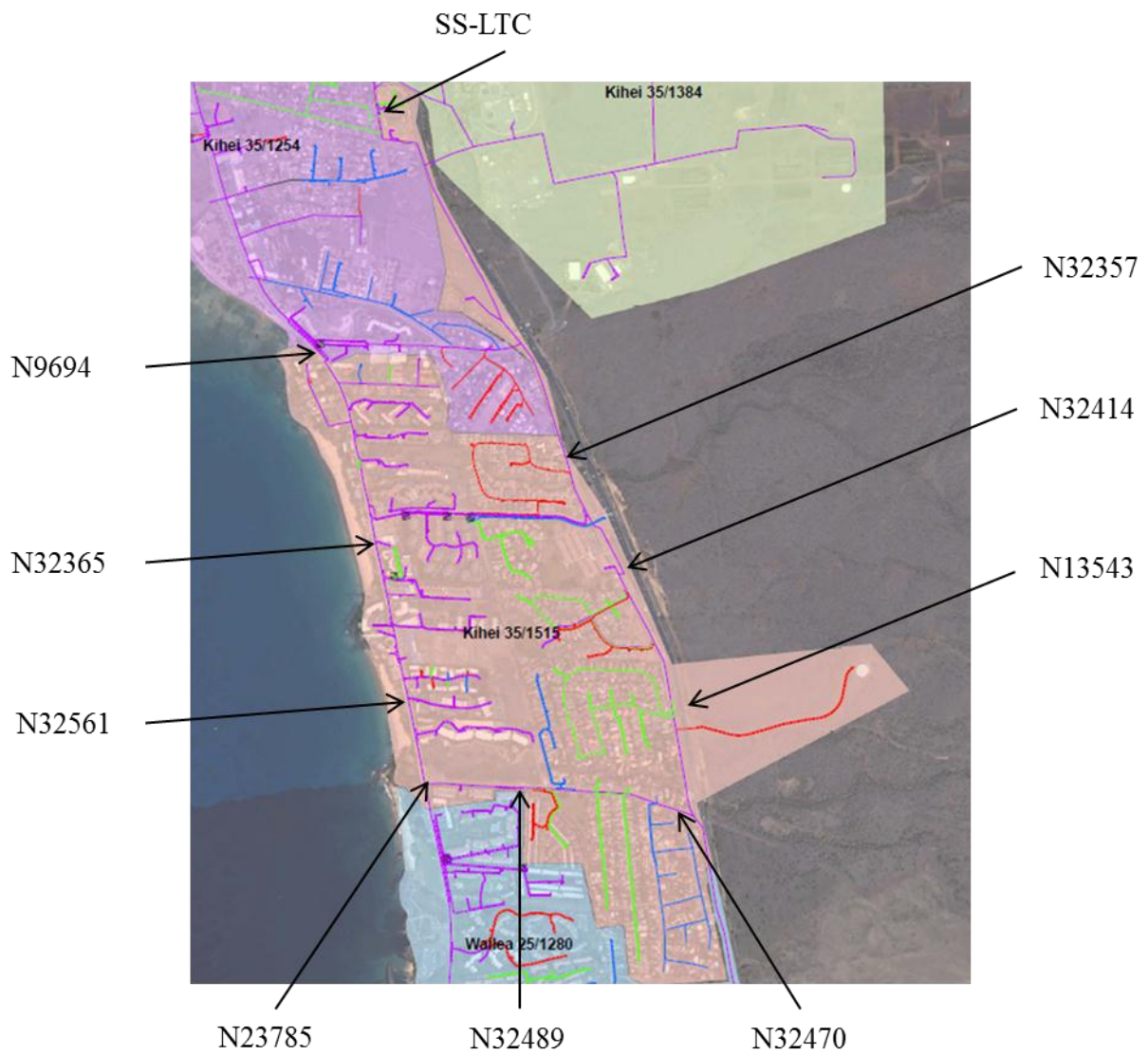


Figure 2.1: Kihei feeder 1515

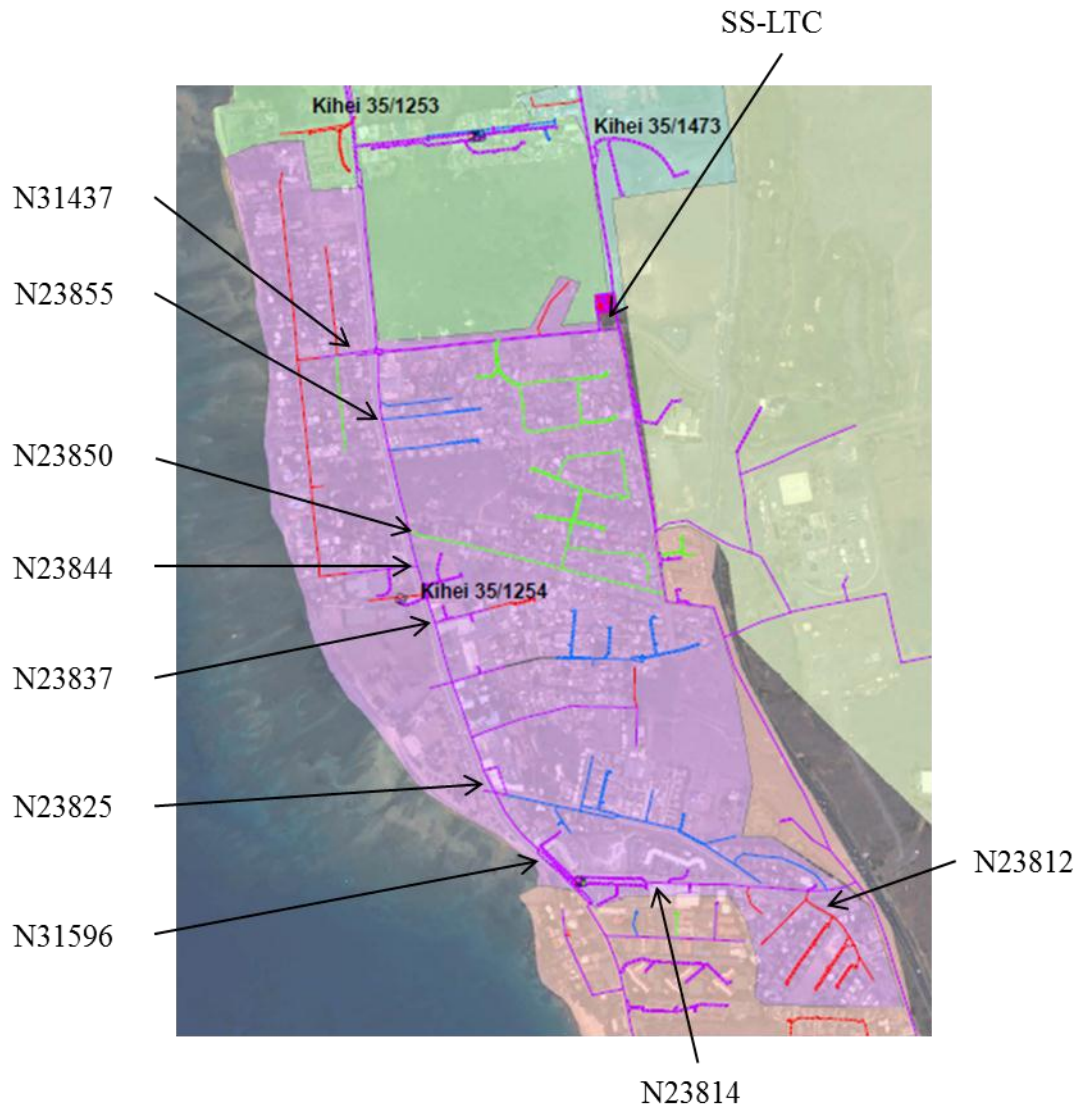


Figure 2.2: Kihei feeder 1254

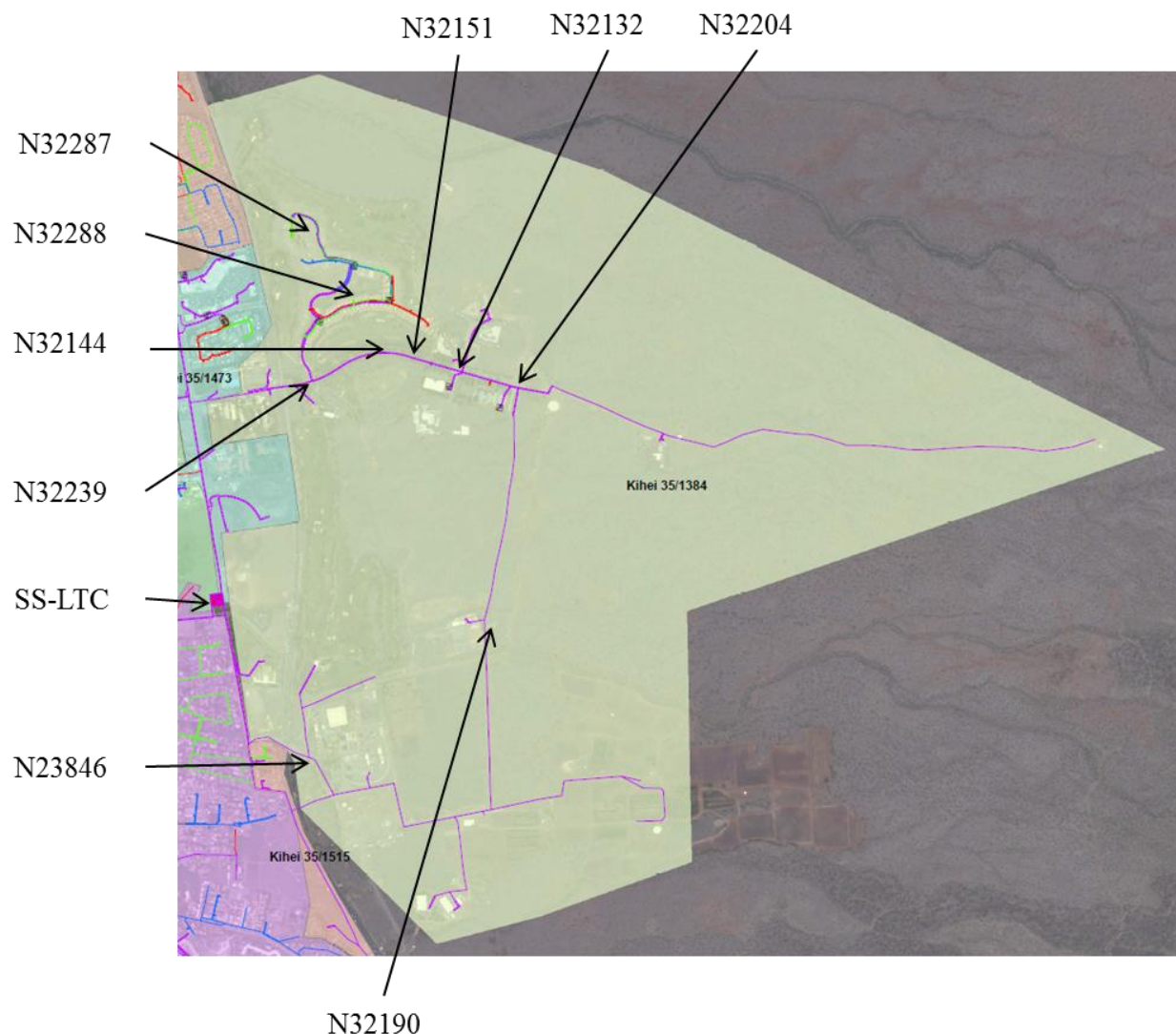


Figure 2.3: Kihei feeder 1384

## 2.1 Base Case Power Profiles

Figure 2.4, Figure 2.5, and Figure 2.6 show the base case power supplied by the transformer and the distributed solar PV for each feeder on February 19<sup>th</sup> 2012. February 19<sup>th</sup> 2012 was selected as a representative day. The plots in the figures were obtained through GridLAB-D simulations that were calibrated to SCADA data provided by MECO. The simulated values differ slightly from the SCADA values because the models were calibrated to provide the best possible representation of the feeder over a three month period, not just a single day. By calibrating over a longer period of time a more accurate model is obtained, and individual SCADA data errors are averaged out.

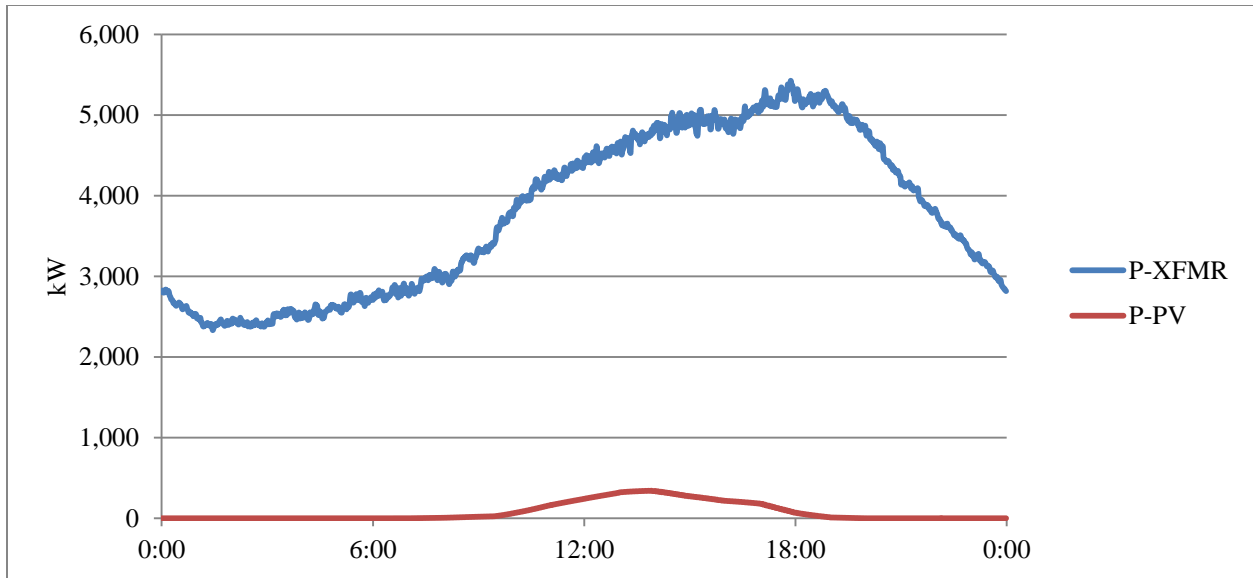


Figure 2.4: Feeder 1515, base case, transformer and PV power, February 19<sup>th</sup>

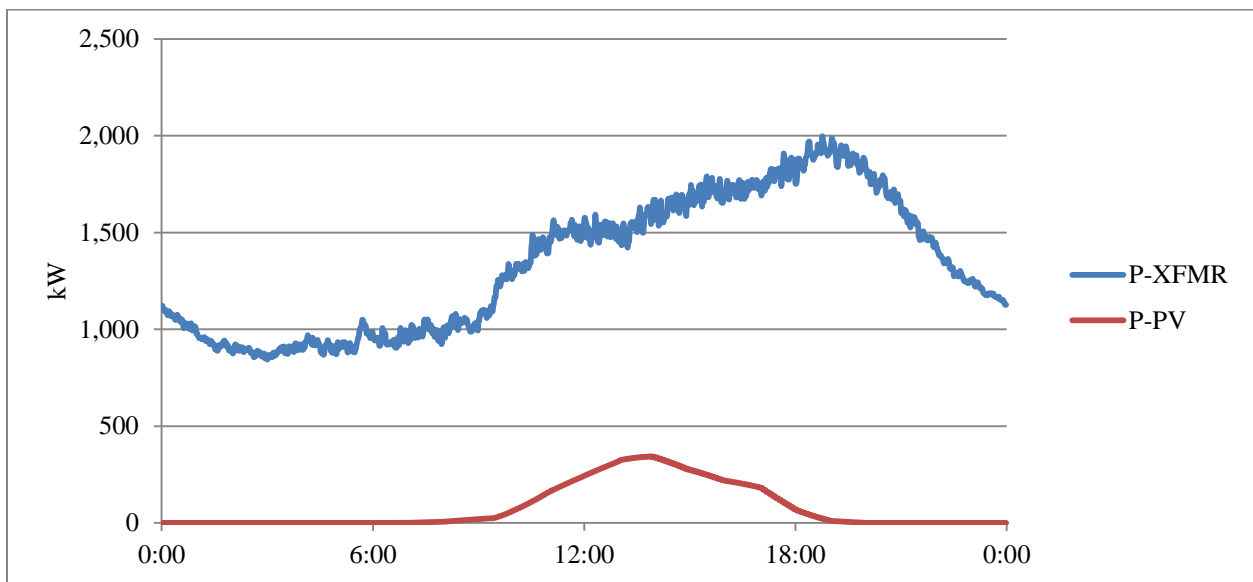


Figure 2.5: Feeder 1254, base case, transformer and PV power, February 19<sup>th</sup>

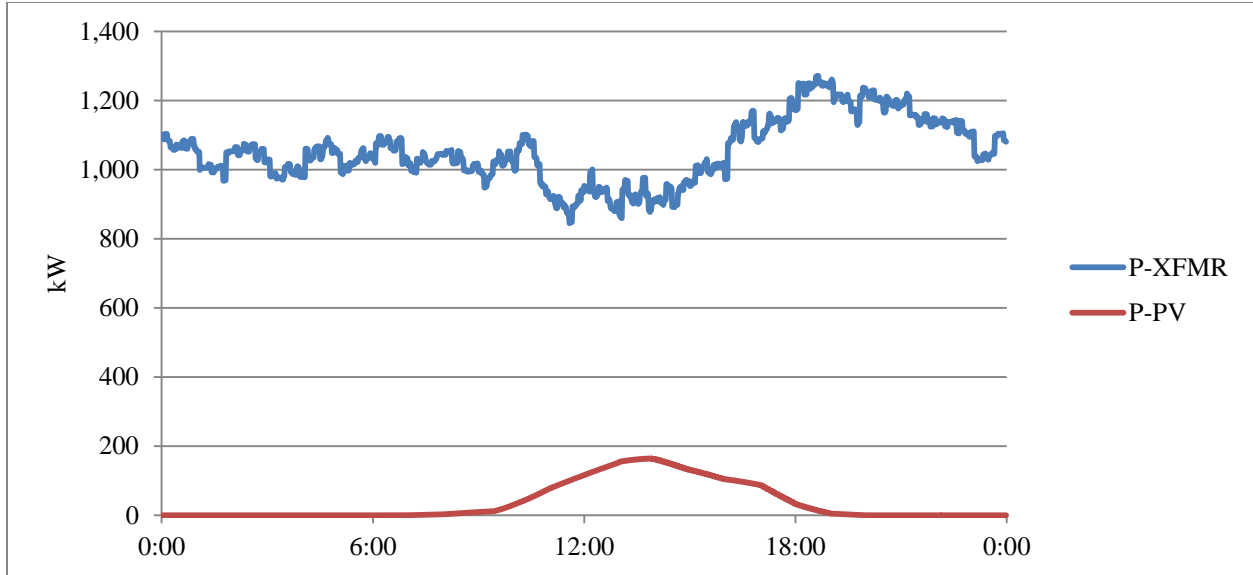


Figure 2.6: Feeder 1384, base case, transformer and PV power, February 19<sup>th</sup>

One key issue to note in the three plots is that the peak solar output is not coincident with the peak feeder load. As a result, the addition of more solar PV systems will not reduce the feeder peak load; it will only reduce the amount of real energy that the substation must provide to the feeder over the course of a day.

## 2.2 Base Case Voltage Profiles

Figure 2.7, Figure 2.8, and Figure 2.9 show the base case voltage profiles for the three Kihei feeders at 17:00 on February 19<sup>th</sup>, 2012. 17:00 was selected because it was near the feeder peak load, with the accompanying high voltage drop. The top and bottom of the voltage scale correspond to the ANSI C84.1 range A values of  $120V \pm 5\%$ . Since these are 12.47 kV feeders with a nominal line to neutral voltage of 7,200V, 114V to 126V on the secondary corresponds to primary voltages of 6,840V to 7,560V.

Each of the three plots starts with the voltage at the output of the substation LTCs (SS-LTC) and progress towards the end of the feeder. All of the listed nodes are on the primary distribution system, at the high side of the secondary service transformers. It would be expected that there would be an additional 2V-3V drop, 120V-180V primary voltage, between the indicated nodes and the end-use point of interconnection. The distances, both physical and electrical, between the ten points listed in the plots are not all equal.

From the three plots, it can be seen that all primary distribution voltages are well within ANSI C84.1 range A. It can be assumed that with standard secondary design practices, the voltages at the point of end-use interconnection will also be with ANSI C84.1 range A, even with the expected 120V-180V drop across the secondary system.

Of the three feeders, 1515 shows the lowest end of line voltage, primarily due to its relatively large and complex size. Between the substation LTC and node N32357, there is a long section of conductor that carries the entire feeder load, resulting in a large voltage drop. At node N32357 the feeder splits, but continues to use the same conductor, so the voltage drops are significantly smaller between subsequent sections.

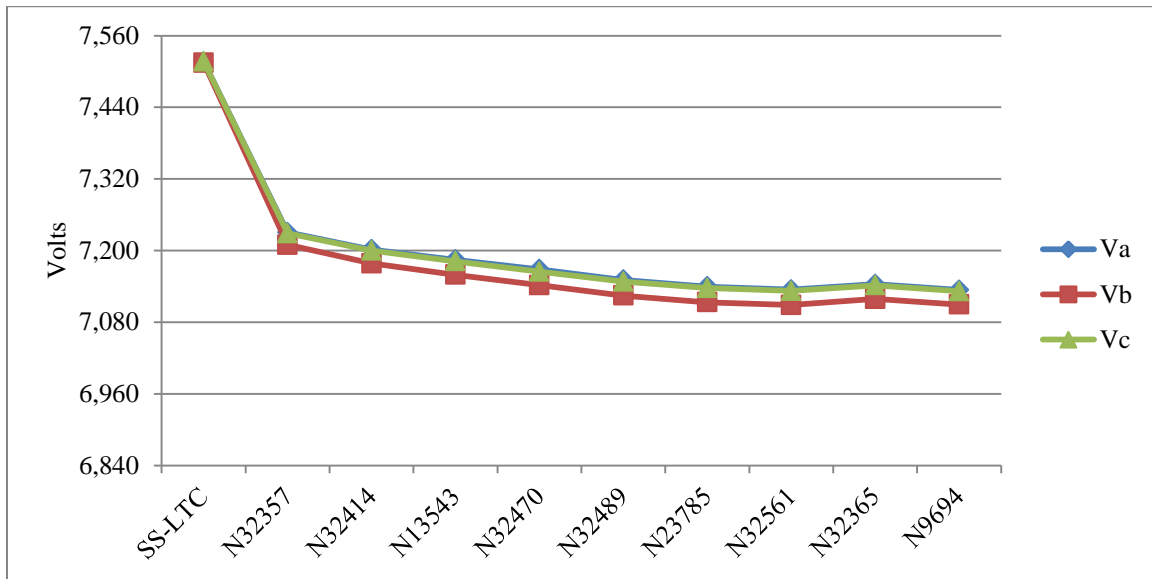


Figure 2.7: Feeder 1515, base case, voltage profile, February 19<sup>th</sup> 17:00

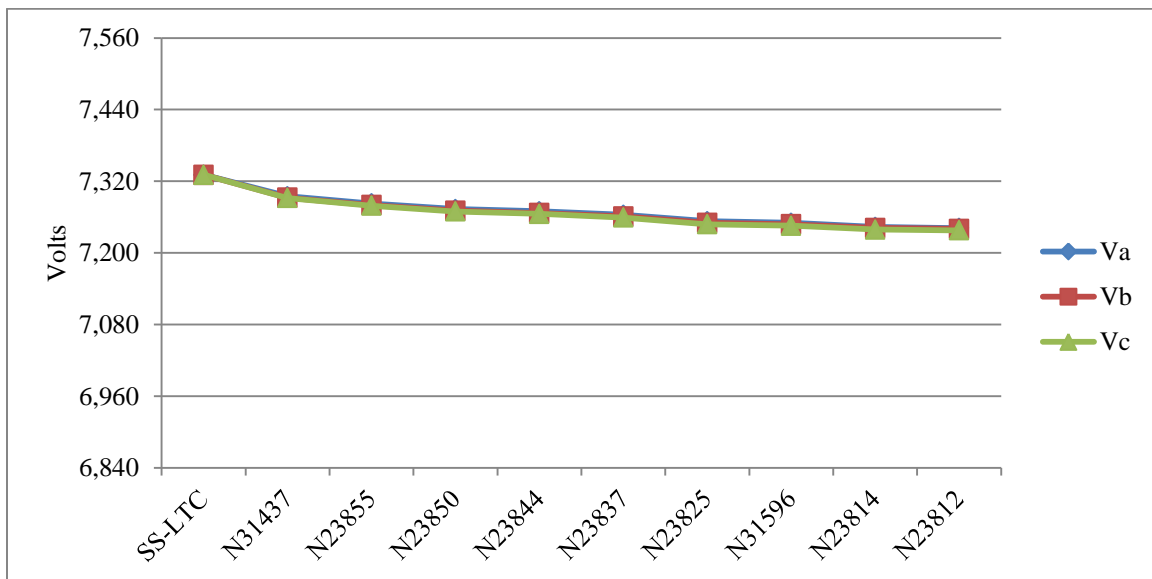


Figure 2.8: Feeder 1254, base case, voltage profile, February 19<sup>th</sup> 17:00

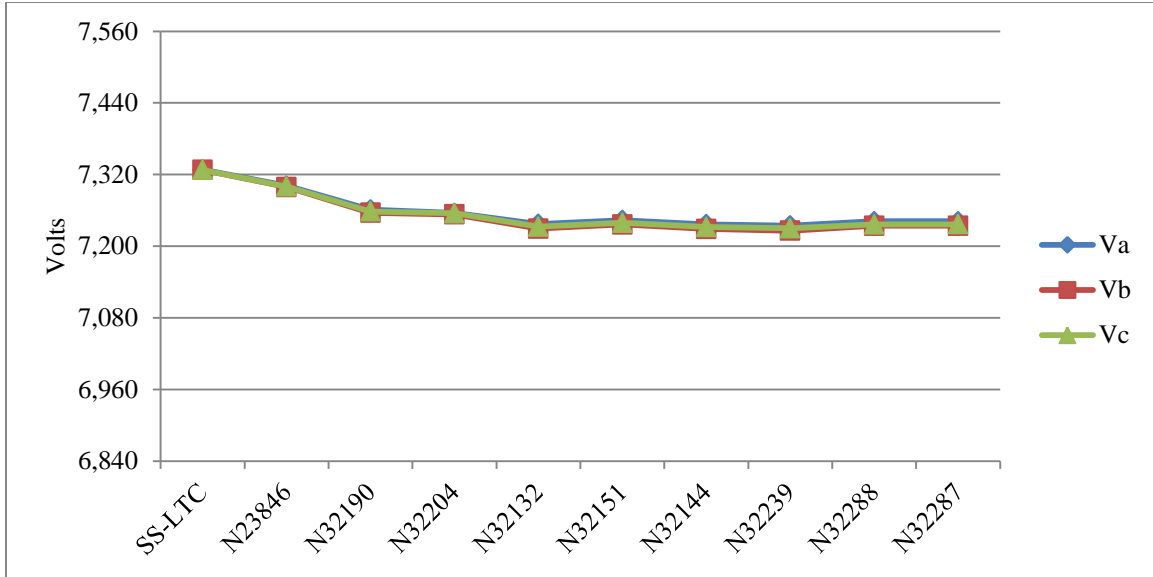


Figure 2.9: Feeder 1384, base case, voltage profile, February 19<sup>th</sup> 17:00

## 2.3 Base Case Time-Series Examination

While section 2.2 examined the voltage profile from the substation LTC to the end of the feeder for a single point in time, the time-series values of voltage for each point over a 24-hour period are equally important. Figure 2.10, Figure 2.11, and Figure 2.12 show the voltage magnitudes at nodes N32561, N31596, and N32249, over a 24-hour period on February 19<sup>th</sup>, 2012.

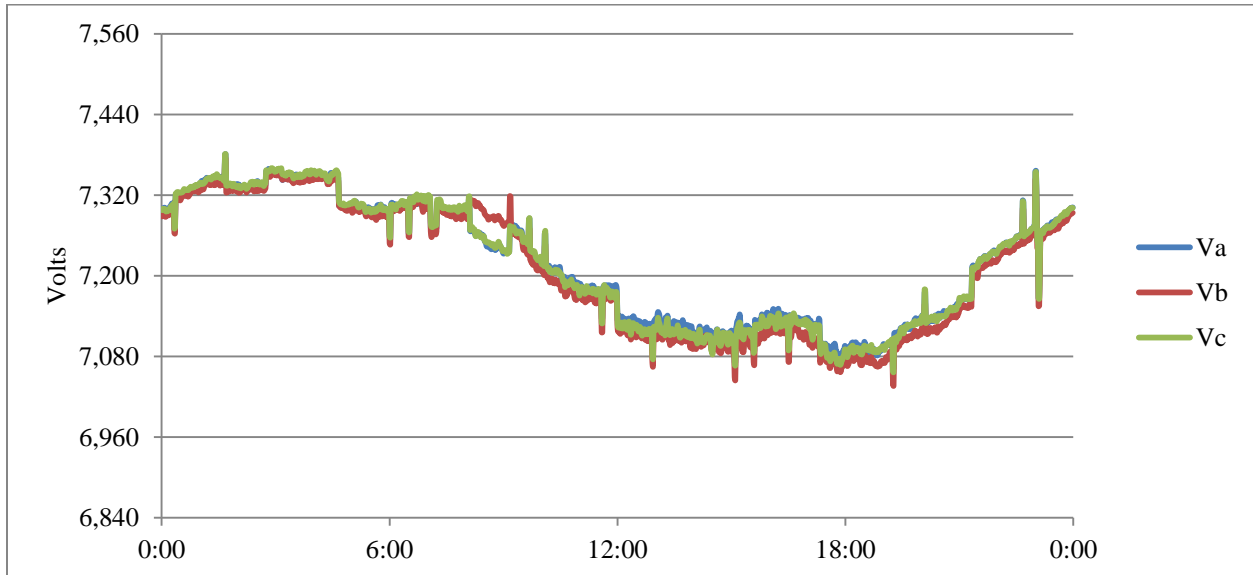


Figure 2.10: Feeder 1515, base case, time-series for node N32561 voltage, February 19<sup>th</sup>



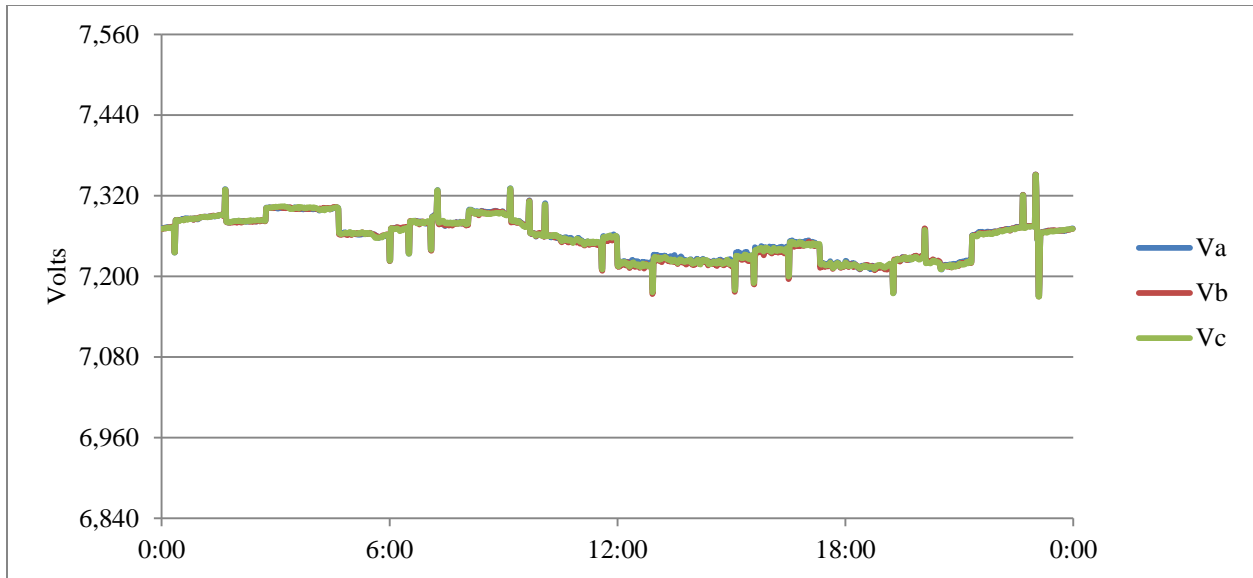


Figure 2.11: Feeder 1254, base case, time-series for node N31596 voltage, February 19<sup>th</sup>

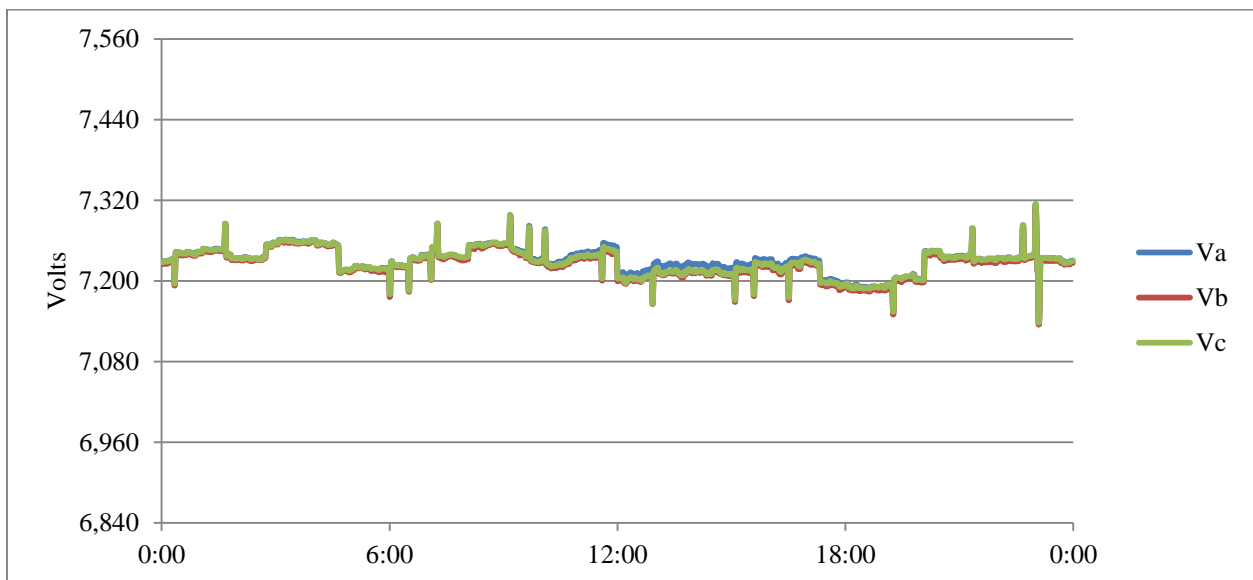


Figure 2.12: Feeder 1384, base case, time-series for node N32239 voltage, February 19<sup>th</sup>

From Figure 2.10, Figure 2.11, and Figure 2.12 it can be seen that over the course of the day there are a number of what appear to be “voltage spikes”. Each spike is in fact two separate events. The first is a step up, or step down, in the 69 kV transmission voltages that were used as boundary conditions in the simulations. These voltage variations are large step changes in voltage and are probably the result of the operation of transmission-level equipment, such as voltage correction capacitors or voltage regulators; the exact cause is not known. The second event is the substation LTC counteracting the large change in voltage, which is greater than the dead band for the LTC’s operation. Because the LTC have a 45-second delay time for operation,



the transmission-level voltage variations are not instantly offset and appear as the voltage spikes shown in the time-series figures.

While the voltage spikes of Figure 2.10, Figure 2.11, and Figure 2.12 are noticeable, it can be seen by observation that they do not move the voltage outside of the ANSI C84.1 range A values. Additionally, the substation LTCs are able to quickly correct for the changes of voltage.

## 2.4 Base Case Concluding Comments

The base case condition for the three Kehei feeders showed no apparent voltage issues due to the existing solar PV units. Both the static, and the time-series simulations, indicated that the voltages remained within the ANSI C84.1 range A values.

### 3 Solar PV Analysis

In the PV analysis for the SIS, a number of different penetration levels for PV are examined. For this report, only the comparison of the base case conditions and a theoretical 50% penetration level for each feeder are shown. 50% penetration indicates that the nameplate capacity of the distributed PV units is equal to 50% of the feeder peak load. The additional PV included for the theoretical 50% penetration case is consistent with the PV that is already installed on the feeders. Additional units in the 50% PV case are residential for 1515, commercial for 1254, and a combination of residential and commercial for 1384. The 50% penetration level case is selected because it represented a significant level of PV that could be reasonably expected to occur in the near future. Higher penetration levels were not examined, but their impacts could be extrapolated.

#### 3.1 50% PV Case Voltage Profiles

In 50% penetration PV case, each of the three Kihei feeders is examined with a hypothetical 50% penetration of PV. Figure 3.1, Figure 3.2, and Figure 3.3 are similar to Figure 2.4, Figure 2.5, and Figure 2.6 in that they show the real power output of the substation transformer, and the distributed solar PV units. The difference is that the amount of peak power provided by the PV is nearly 50% of the peak feeder load. While the name plate capacity of the PV units is 50% of the feeder peak load, the actual power output of the units is slightly lower because of factors such as non-optimal solar tracking, dirty solar panels, and inverter inefficiencies. Non-optimal tracking is a realistic assumption since most residential and commercial PV units are fixed units with no tracking capabilities.

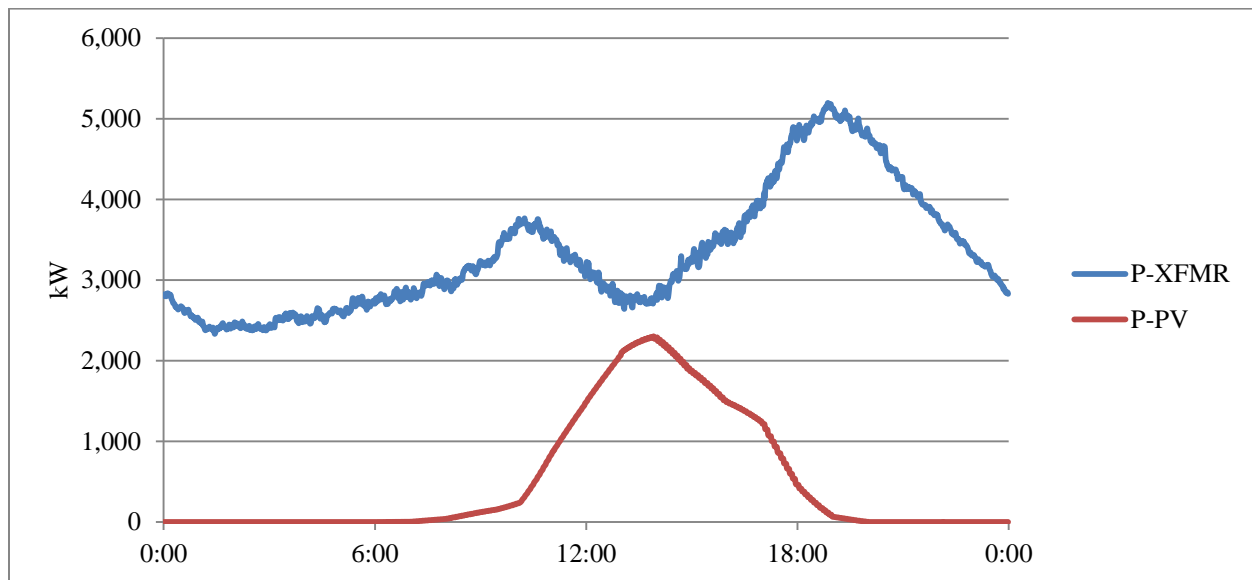


Figure 3.1: Feeder 1515, 50% PV case, transformer and PV power, February 19<sup>th</sup>

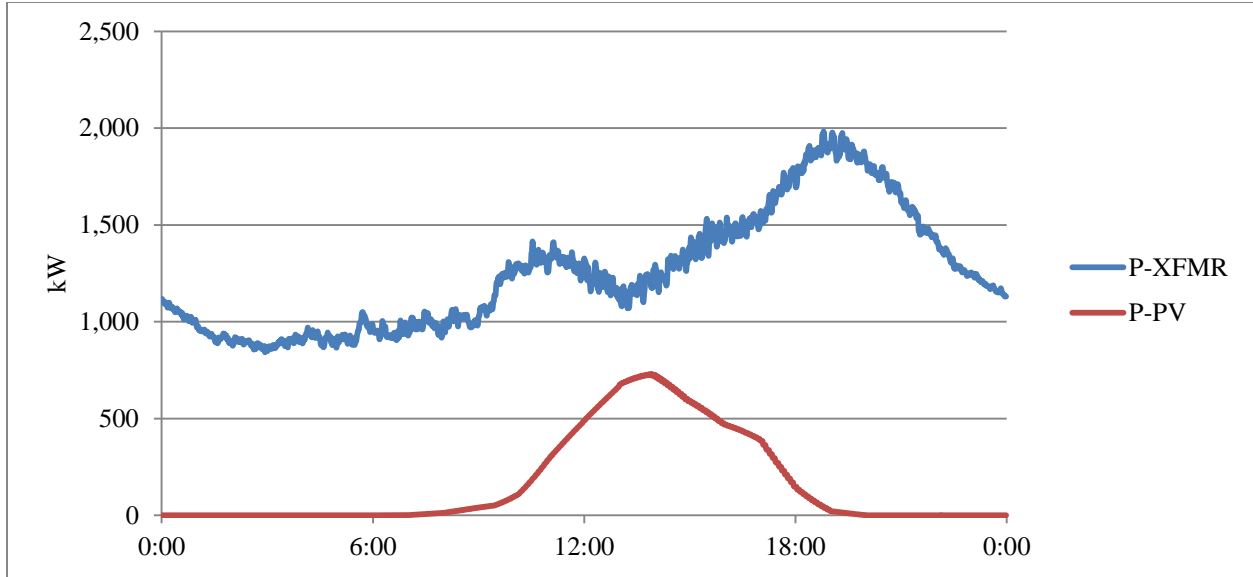


Figure 3.2: Feeder 1254, 50% PV case, transformer and PV power, February 19<sup>th</sup>

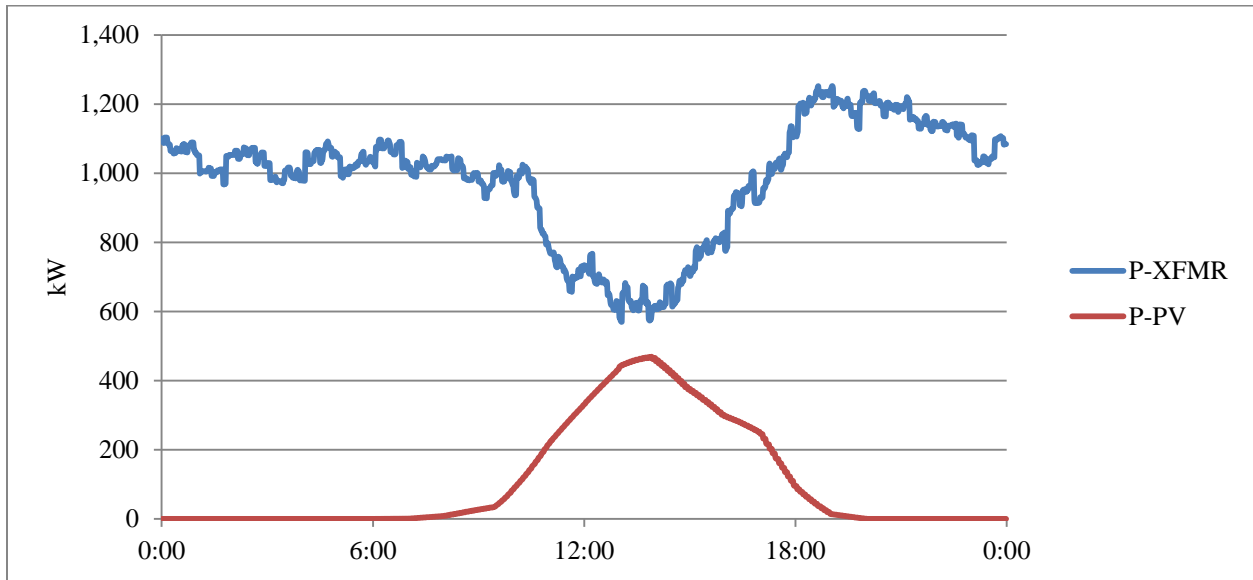


Figure 3.3: Feeder 1384, 50% PV case, transformer and PV power, February 19<sup>th</sup>

In the 50% penetration case, shown in the previous three plots, it can be seen that similar to the base case, the solar PV does not provide full output power during the peak load time. In fact, the solar PV output is at a very low level by the peak load time. This can be attributed to the fact that PV units are generally designed to capture the maximum amount of energy, not reduce the feeder peak. Consequently, the tilt angle of most units is set so that it captures the maximum amount of solar radiation near noon, resulting in a suboptimal angle for times later in the day. The actual peak solar output occurs only an hour or two before sunset.

### 3.2 50% PV Case Voltage Profiles

Figure 3.4, Figure 3.5, and Figure 3.6 show the voltage profiles for the 50% PV case. It can be seen that there is only a minor difference between the voltage profiles for the base case and the 50% PV case. This is primarily due to two facts: first, the PV inverters are only outputting real power, and second, the substation LTCs will correct for any large deviations.

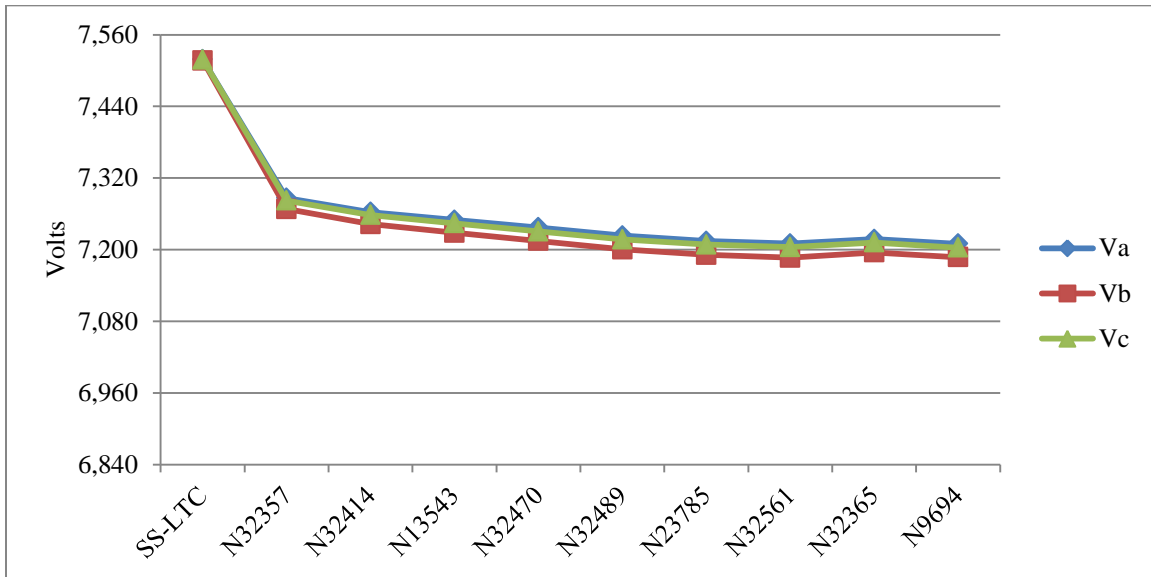


Figure 3.4: Feeder 1515, 50% PV case, voltage profile, February 19<sup>th</sup> 17:00

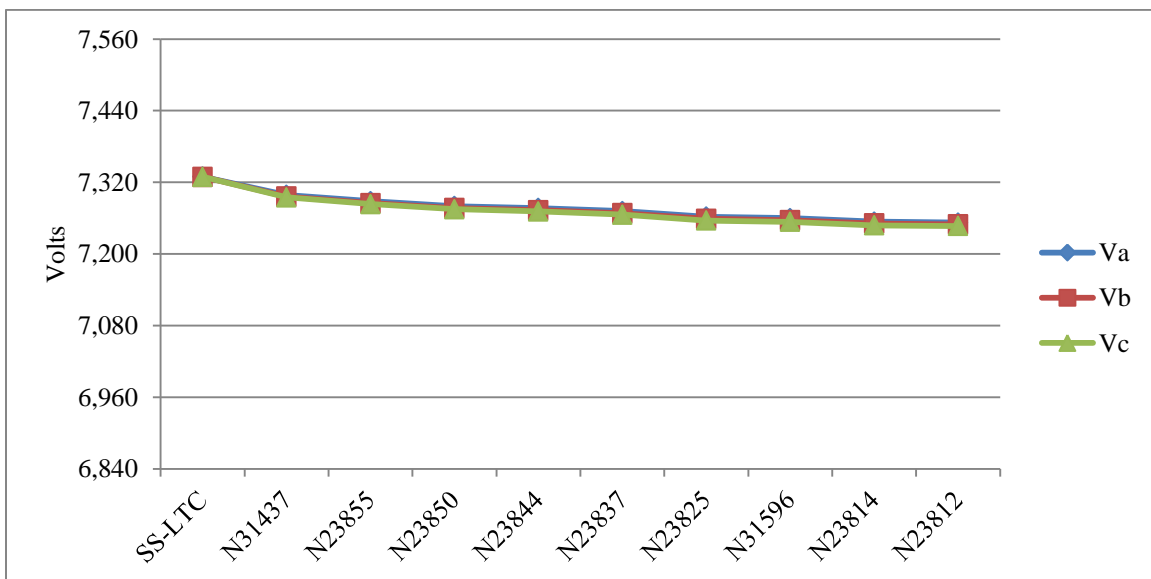


Figure 3.5: Feeder 1254, 50% PV case, voltage profile, February 19<sup>th</sup> 17:00

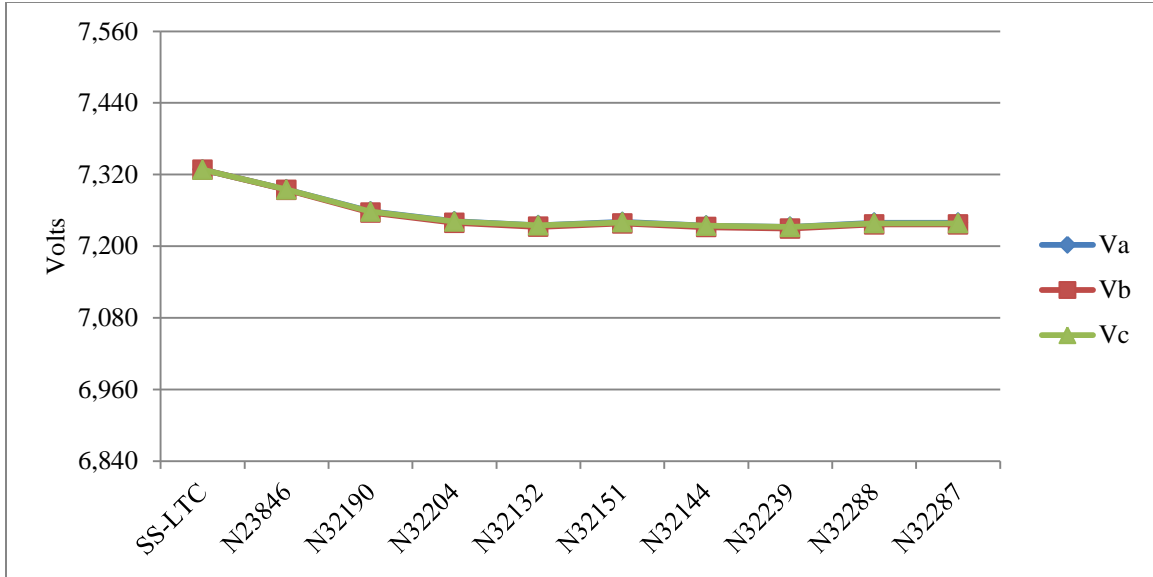


Figure 3.6: Feeder 1384, 50% PV case, voltage profile, February 19<sup>th</sup> 17:00

### 3.3 50% PV Case Time-series Examination

In the previous section, it was shown that the 50% PV case does not cause any observable problems with the voltage profile across the feeder. The next step is to examine the time-series values at a select node over a 24-hour period, which will indicate if there are any voltage problems over the diurnal cycle. Figure 3.7, Figure 3.8, and Figure 3.9 plot the difference in voltage between the base case and the 50% case for the 3 Kihei feeders: 1515, 1254, and 1384 respectively. The values are positive because the 50%

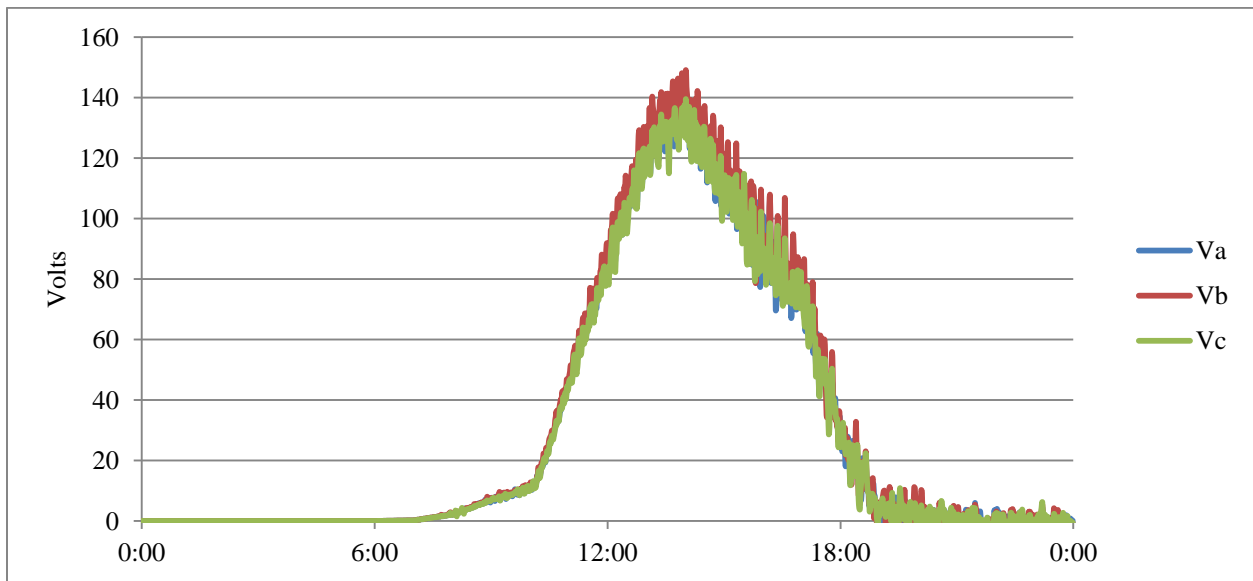


Figure 3.7: Feeder 1515, difference of base case and 50% PV case, time-series voltage at node N32561, February 19<sup>th</sup>

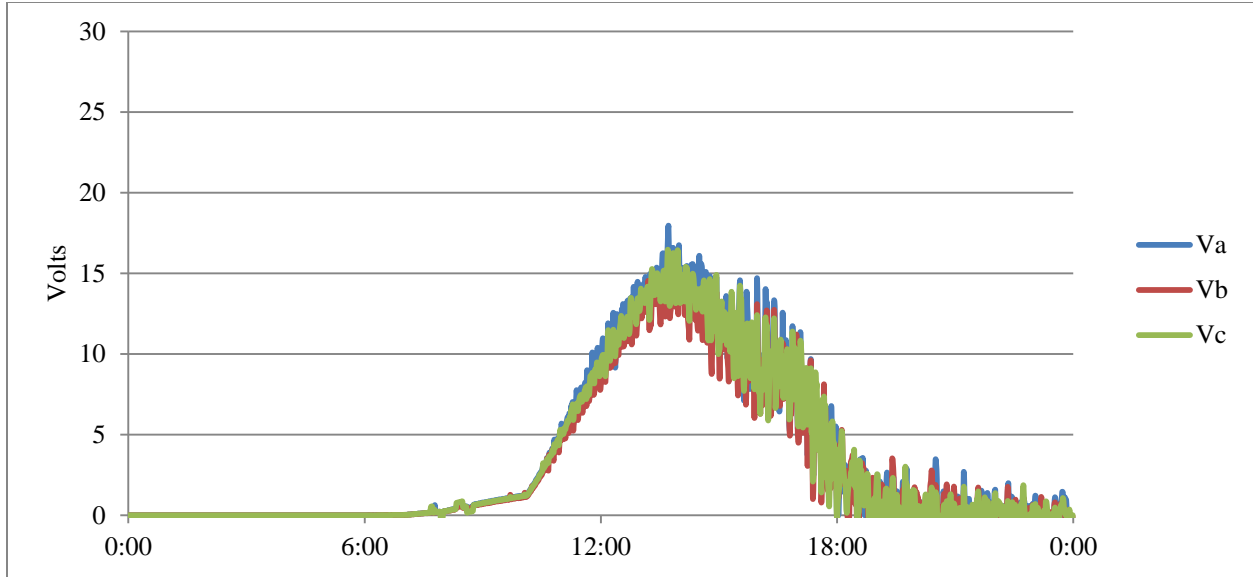


Figure 3.8: Feeder 1254, difference of base case and 50% PV case , time-series voltage at node N31596, February 19<sup>th</sup>

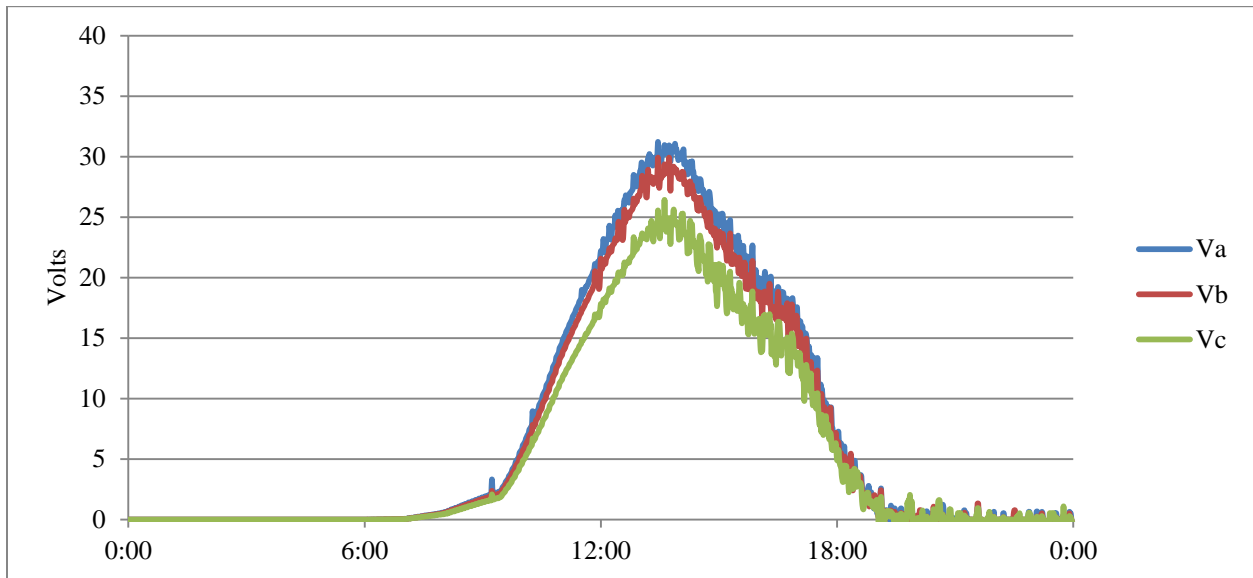


Figure 3.9: Feeder 1384, difference of base case and 50% PV case, time-series voltage at node N32239, February 19<sup>th</sup>

One last point of interest between the base case and the 50% PV case is the impact on the power factor at the substation. Figure 3.10 shows the feeder level power factor for the base case and the 50% PV case. It can be seen that the power factor for the 50% case is noticeably lower than the power factor for the base case during the peak solar output time frame. This can be attributed to the fact that the PV inverters are operating at unity power factor, requiring the substation to provide less real power and the same amount of reactive power.

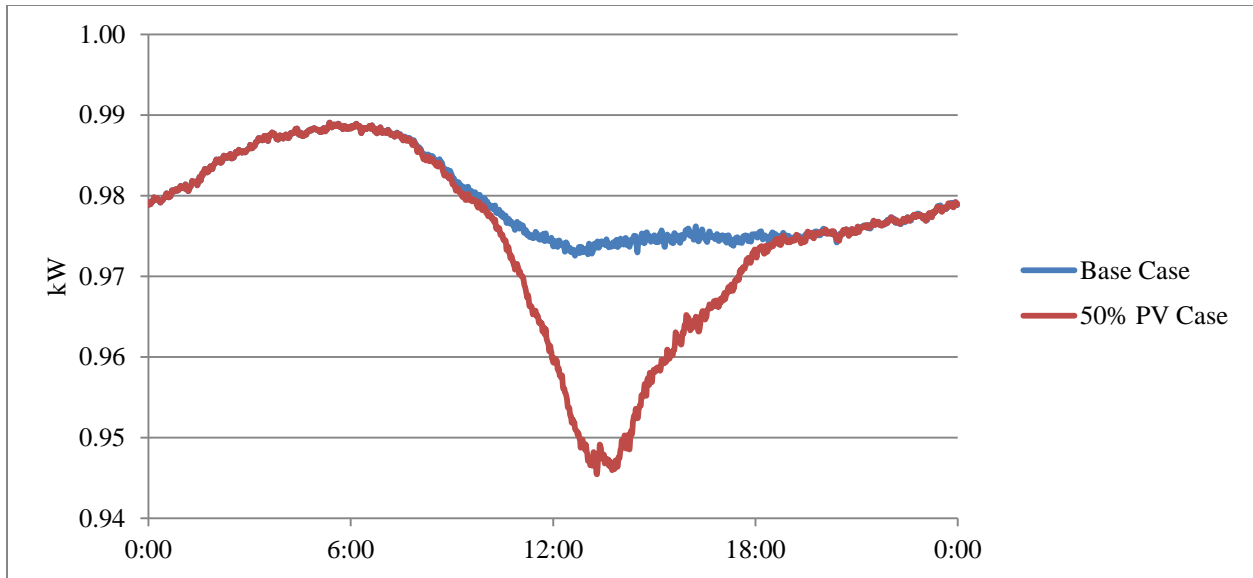


Figure 3.10: Feeder 1515, comparison of base case and 50% PV case, power factors, February 19<sup>th</sup>

### 3.4 50% PV Case with Cloud Transient

The cloud transient simulations are performed with a 1-second minimum time step. The cloud transient is modeled as a decrease in the direct solar insolation from 100% to 20% in 5 seconds, with a return to 100% after 1-minute. Since simulations of the three feeders produced similar results, only feeder 1515 will be examined. Figure 3.11 shows the time-series values of voltage at node N32561 for the base case scenario. From Figure 3.11 it can be seen that the solar transient causes a slight drop in the voltage. The voltage drop is highlighted in Figure 3.12 which shows the difference between the case without the transient and the base case with the transient.

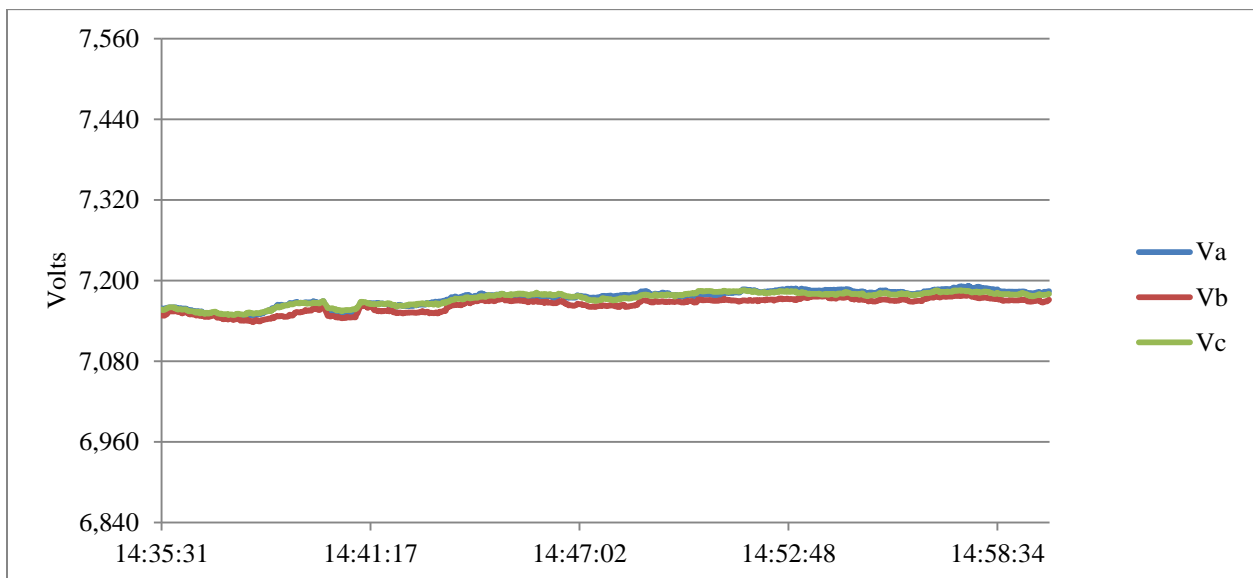


Figure 3.11: Feeder 1515, base case with 1-minute cloud transient, voltage at node N32561, February 19<sup>th</sup> 14:35-15:00

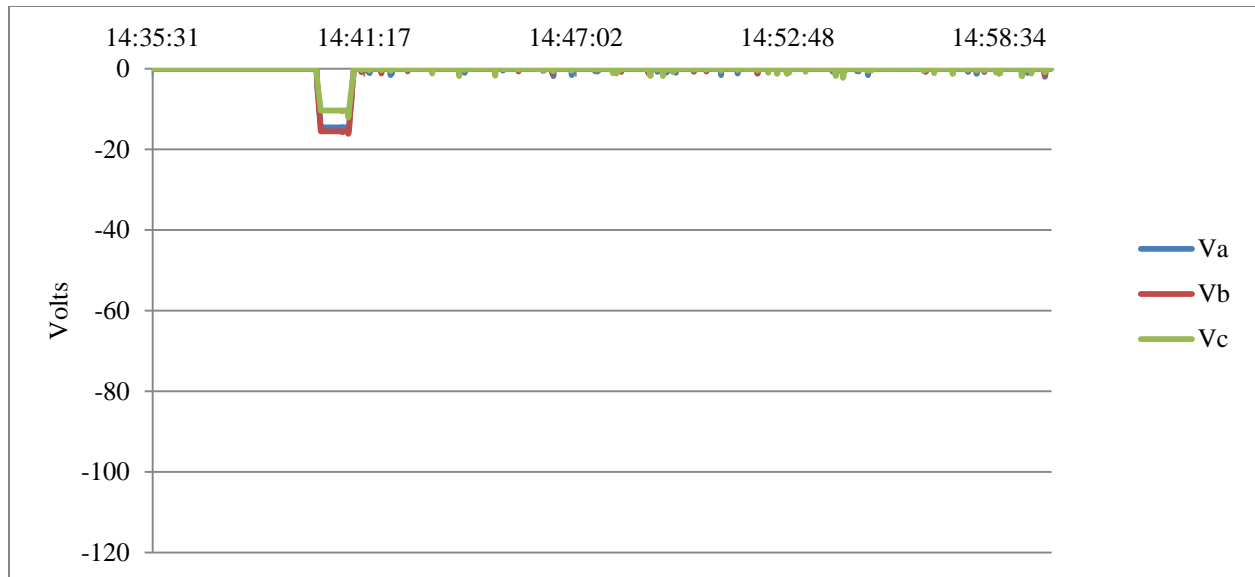


Figure 3.12: Feeder 1515, difference of base case with and without 1-minute cloud transient, voltage difference at node N32561, February 19<sup>th</sup> 14:35-15:00

Figure 3.13 and Figure 3.14 are similar to Figure 3.11 and Figure 3.12, except that they are for the 50% PV case instead of the base case. From the figures, it is clear that there is a significantly larger voltage drop for the 50% PV case. Even with the greater drop in voltage during the transient, there is still no concern that ANSI standards will be violated.

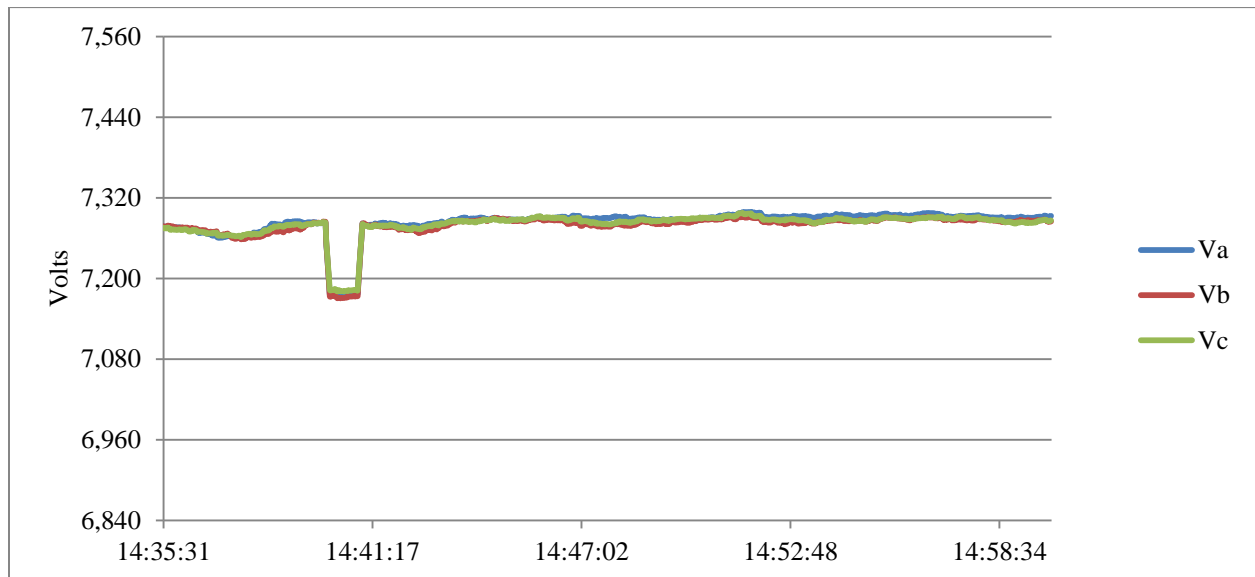


Figure 3.13: Feeder 1515, 50% PV case with 1-minute cloud transient, voltage at node N32561, February 19<sup>th</sup> 14:35-15:00



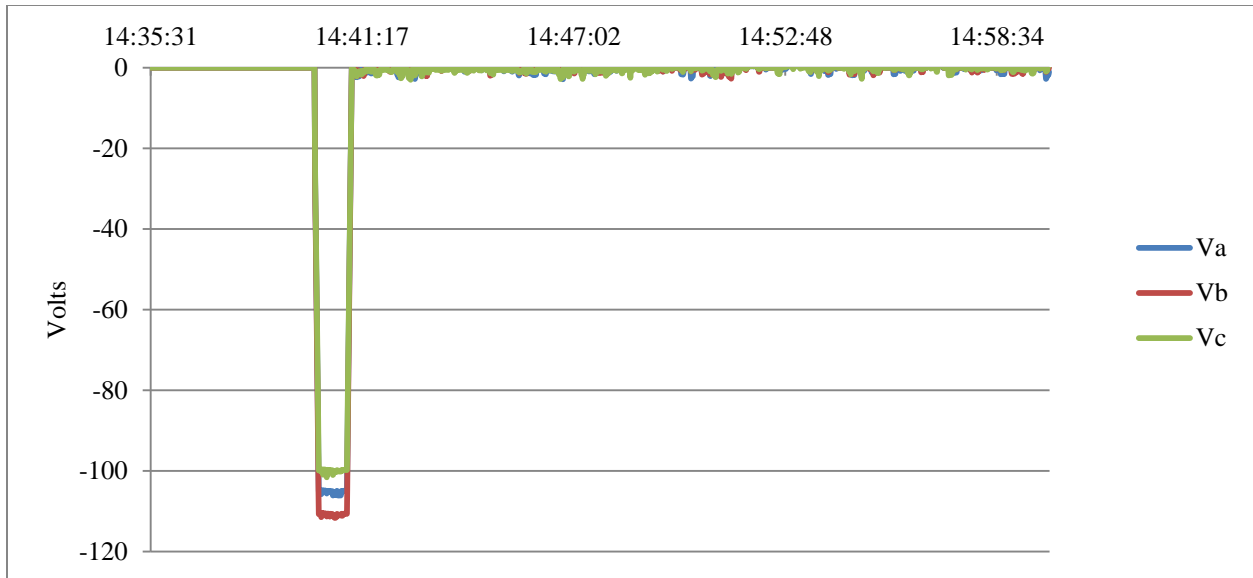


Figure 3.14: Feeder 1515, difference of 50% PV case with and without 1-minute cloud transient, voltage difference at node N32561

### 3.5 PV Concluding Comments

In this section of the SIS a theoretical 50% PV case has been examined, and its impacts on the system have been compared to the base case. Simulations were conducted with a 1-minute minimum time step for a full 24 hours to examine the diurnal voltage variations. Additional simulations with a 1-second time step for 30 minutes were run to examine the voltage impact of a large cloud crossing event, a cloud transient. In both sets of simulations, it was shown that the existing voltage control devices, specifically the substation LTCs, were able to maintain the voltage within the ANSI band. Despite this, large cloud transients that occur more quickly than the response time of the LTCs, have the potential to produce voltage variations that are noticeable to end-use customers. This most common manifestation of these voltage variations would be in a slight change in brightness of incandescent lights, and this would only be noticeable if the end-use customer were paying particular attention at the time of the transient. Even the most direct impacts of the 50% PV case would have no discernible impact on the end-use customers.

## 4 EV Analysis

A goal of the Japan U.S. Island Grid Project is to examine the feasibility of using EVs as a form of distributed energy storage to offset the variability of transmission-level wind resources. This section of the SIS will focus on the potential impacts of high penetration levels of EVs that are used to offset transmission-level variability. The impacts of EVs that will be examined are the loading of service transformers and voltage impacts at the feeder level. The specific method by which the EVs are used to regulate transmission level wind resources will not be examined in the SIS.

### 4.1 Individual Transformer Impacts

The first part of the EV analysis will focus on the impacts of EVs at the service transformer level. Unlike at the feeder level where load diversity results in a “smooth” load profile, at the service transformer level, the load profile appears more “jagged” due to a lack of load diversity. Figure 4.1 shows the simulated loading of a single 25 kVA service transformer that is serving 9 residential houses. The 9 houses are connected to the 25 kVA transformer via separate 1/0 triplex cable.

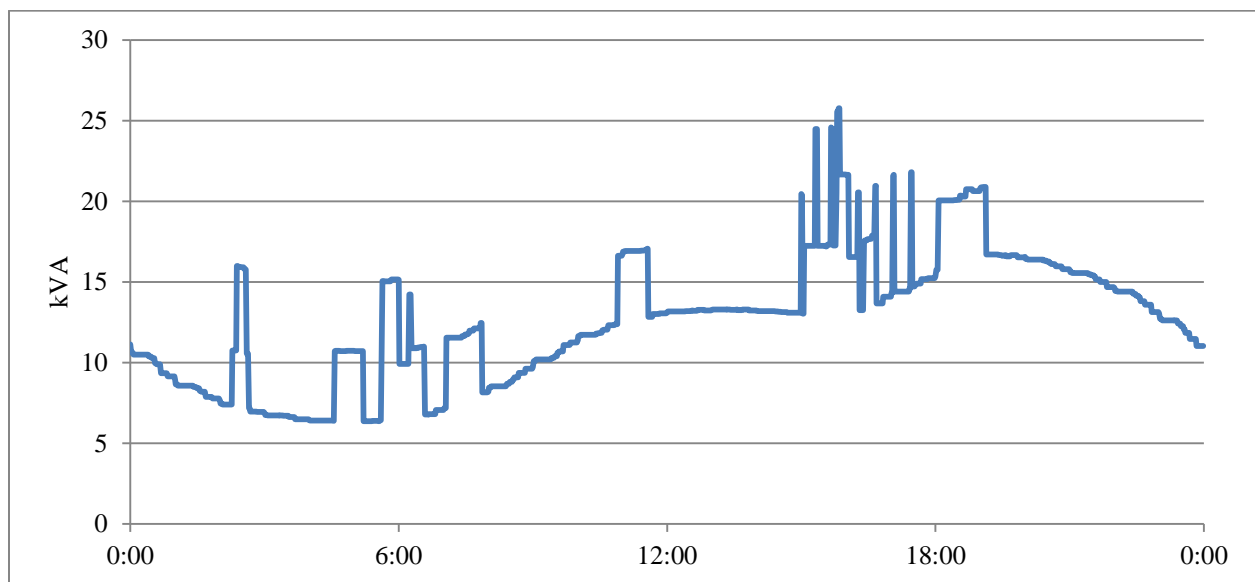


Figure 4.1: Base case, apparent power loading of a single 25 kVA service transformer, February 19<sup>th</sup>

The load level in Figure 4.1 is generated using the GridLAB-D simulation environment, as discussed in Appendix A. At each of the houses large loads such as HVAC and hot water heating are individually modeled, while smaller loads such as plug loads and lighting are modeled as an average value. For the purposes of the SIS, HVAC is a broadly used term and it includes formal commercial HVAC systems and residential window mounted air conditioning units.

This combination of load models results in a time-varying base load combined with large individual loads that can cause load spikes. In Figure 4.1, the load spikes are all due to either HVAC or hot water heating.

The coincidental operation of large loads in separate houses can cause a normally moderately-loaded transformer to become over loaded. This can be seen in Figure 4.1 where the 25 kVA rating of the secondary transformer is momentarily exceeded at approximately 15:50 P.M. While this is a violation of the transformer rating, it is only momentary and will have a negligible impact on the unit's life. A more significant problem is when the transformer rating is exceeded for a prolonged period of time. Because transformer ratings are based on thermal limits, it is necessary for them to either operate continuously below their nameplate rating, or to have a cool-down period after an extended overload. The charging of EVs can prevent the night time cool down of the transformer because they tend to charge at night.

Figure 4.2 shows the load on the same transformer shown in Figure 4.1, and it includes another curve for a 50% penetration of EVs. A 50% penetration level of EVs corresponds to approximately 4 units, each with a maximum charging capacity of 3.3 kW, for a combined total of slightly more than 50% of the transformer nameplate capacity. In this case, it can be seen that the EVs do not increase the peak load because they are primarily charging in the evening; it is assumed that there is no mid-day charging. As a result, the peak load is unchanged, but the transformer average load level had increased, with the entire increase occurring in the evenings. Since the transformer only experiences a single momentary overload, a 50% penetration of EVs will not significantly impact the lifetime of the service transformer.

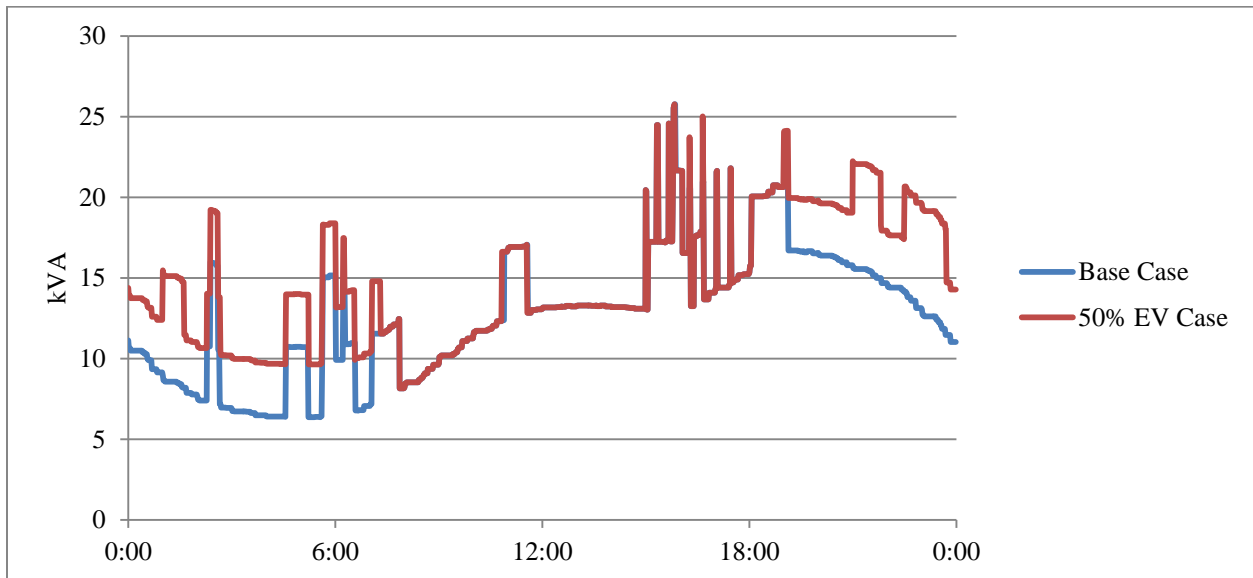


Figure 4.2: 25 kVA transformer, comparison of base case and 50% EV case, apparent power, February 19<sup>th</sup>

Unlike some technologies that are deployed uniformly on a distribution system, EVs tend to be deployed in clusters. Because of social and economic factors, it is very likely that a large number of EVs could be supplied by a small number of service transformers, while the majority of service transformers on a feeder are supplying no EVs.

Figure 4.3 is similar to Figure 4.2, except that it compares the base case and a 100% penetration of EVs. The 100% penetration case corresponds to 8 EVs, each with a charging capacity of 3.3 kW, and a total charging capacity of 26.4 kW, which is slightly over 100% of the transformer rating. Once again the charging is primarily in the evening. In the 100% penetration case, a new peak occurs at approximately 3:00 A.M. and the transformer is operated near its nameplate capacity for the majority of the evening. In this case, a measurable decrease in the operating life of the service transformer would be expected. At this penetration level, a larger service transformer should be installed.

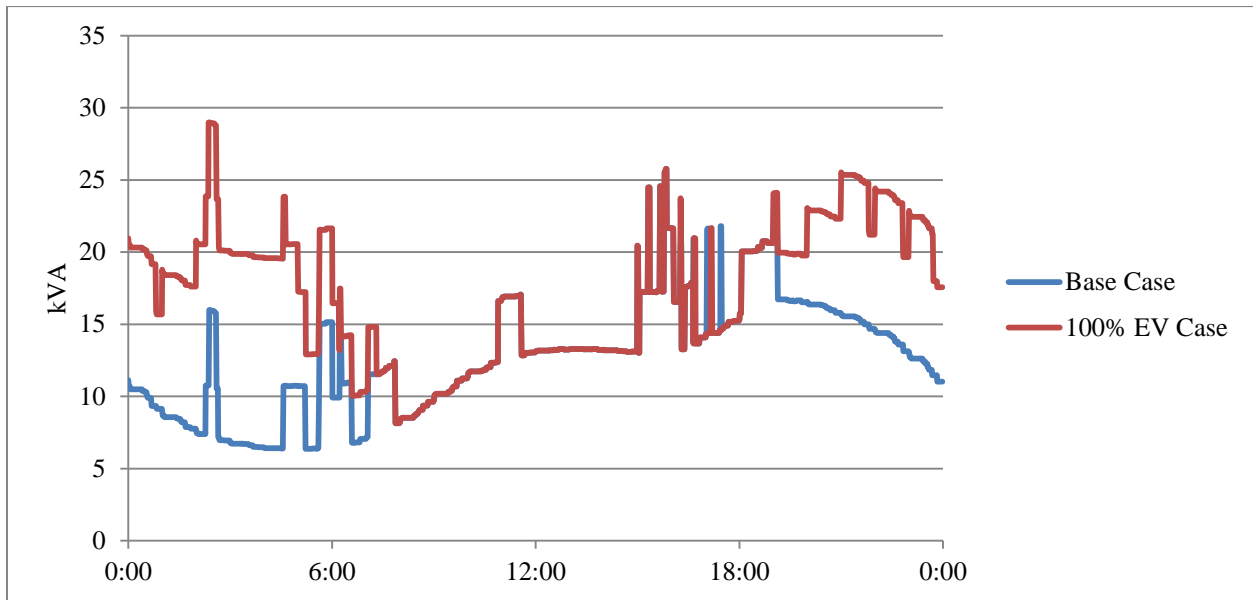


Figure 4.3: 25 kVA transformer, comparison of base case and 100% EV case, apparent power, February 19<sup>th</sup>

Figure 4.4 shows a 150% penetration of EVs that corresponds to 12 EVs, each with a charging capacity of 3.3 kW. In this case, the transformer nameplate capacity is continually exceeded in the evenings and the service life of the unit would be significantly reduced. The magnitude of the service life reduction would depend on the specific heat dissipation characteristics of the transformer in addition to other design specifications. The 150% penetration case is included as an illustrative example; it is not expected that a utility would allow a transformer to be overloaded to this level for an extended duration.

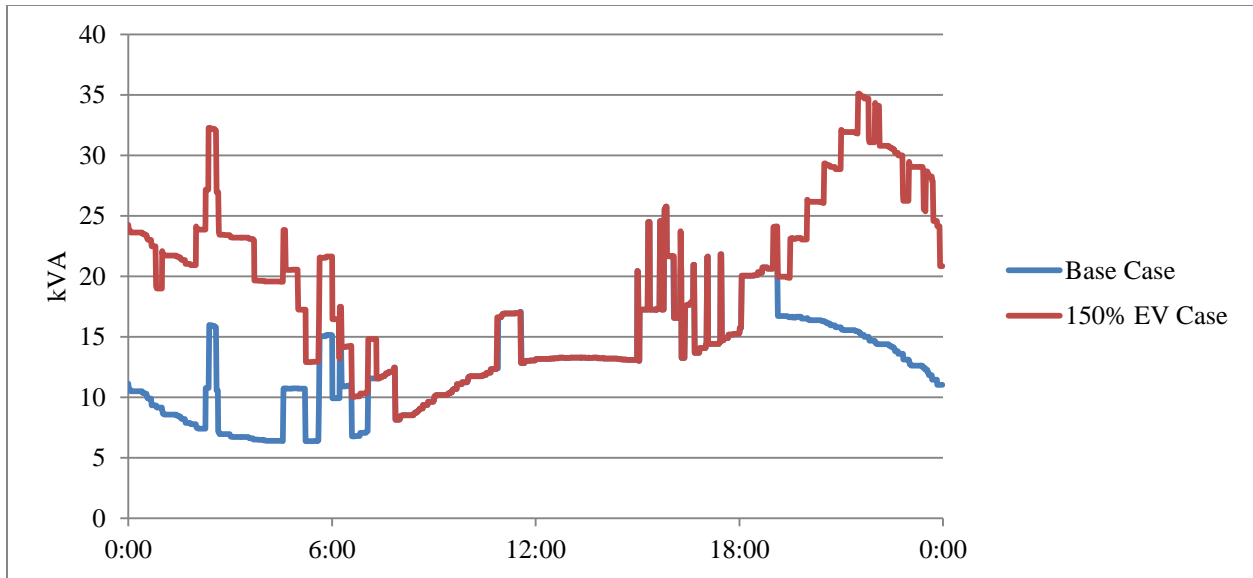


Figure 4.4: 25 kVA transformer, comparison of base case and 150% EV case, apparent power, February 19<sup>th</sup>

## 4.2 Distribution Feeder Impacts

In the previous section, 50%, 100%, and 150% EV penetration scenarios were examined at the service transformer level. At the distribution feeder level, it is unlikely that anything approaching these levels will be encountered for at least the next 10 years. For the purposes of the SIS, feeder level penetration levels of 5%, 25%, and 50% were examined for feeder 1515. Feeder 1515 was selected since it is primarily a residential feeder. Figure 4.5, Figure 4.6, and Figure 4.7 show the real power supplied by the substation for the base case and 5%, 25%, and 50% penetration of EVs, respectively. The 5%, 25%, and 50% penetration cases correspond to 111, 555 and 1109 EVs, respectively.

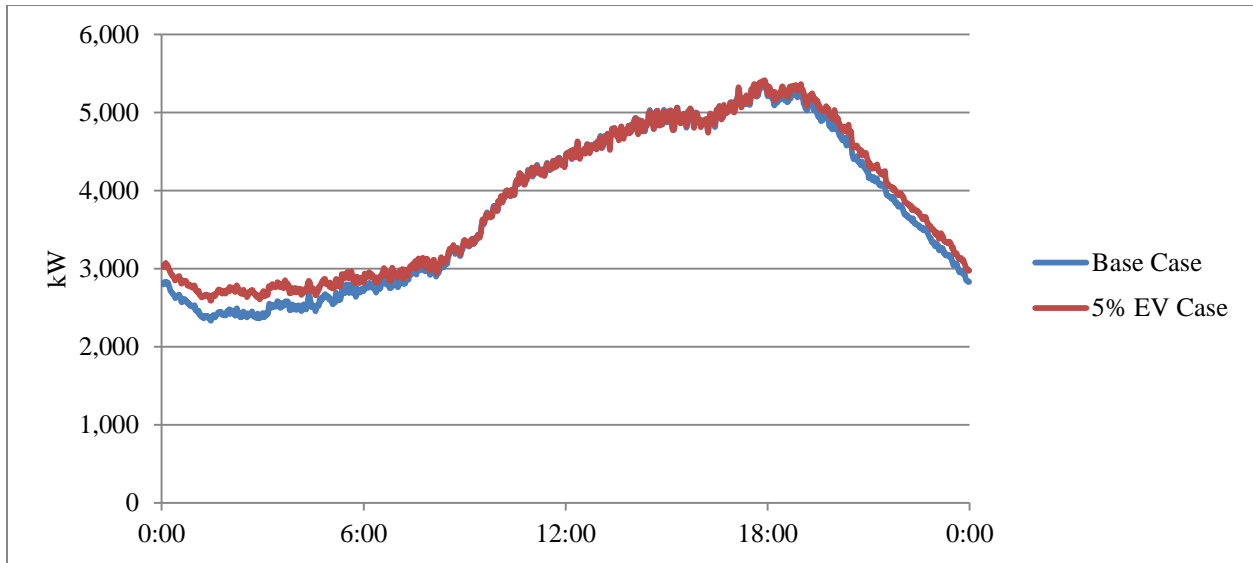


Figure 4.5: Feeder 1515, comparison of base case and 5% EV case, real power, February 19<sup>th</sup>

From Figure 4.5 it can be seen that there is an increase in night time, off-peak loading and little-to-no impact on the peak load. Other than a slightly higher night time load, a 5% penetration of EVs has a minimal impact on the power that must be supplied from the substation. A constant peak load, with a corresponding off-peak increase could complement transmission level wind power.

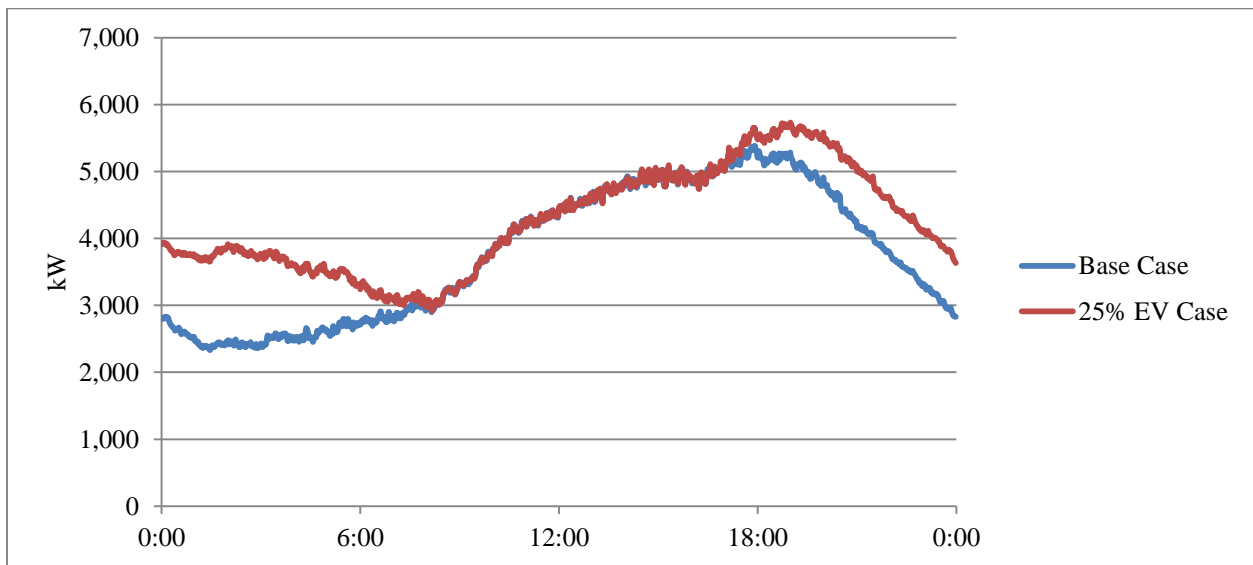


Figure 4.6: Feeder 1515, comparison of base case and 25% EV case, real power, February 19<sup>th</sup>

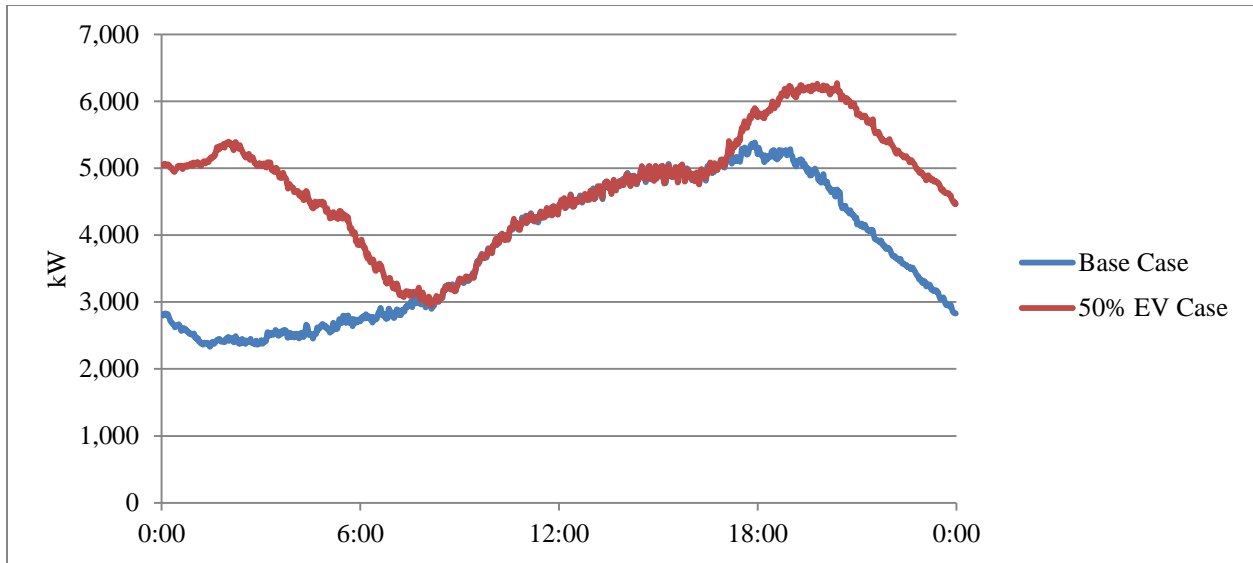


Figure 4.7: Feeder 1515, comparison of base case and 50% EV case, real power, February 19<sup>th</sup>

In both the 25% and 50% penetration cases, Figure 4.6 and Figure 4.7, the peak load, as well as the off-peak load, increase dramatically. For the 50% case, it is possible that a new substation transformer would need to be installed, especially if this penetration level existed on multiple feeders supplied by the substation.

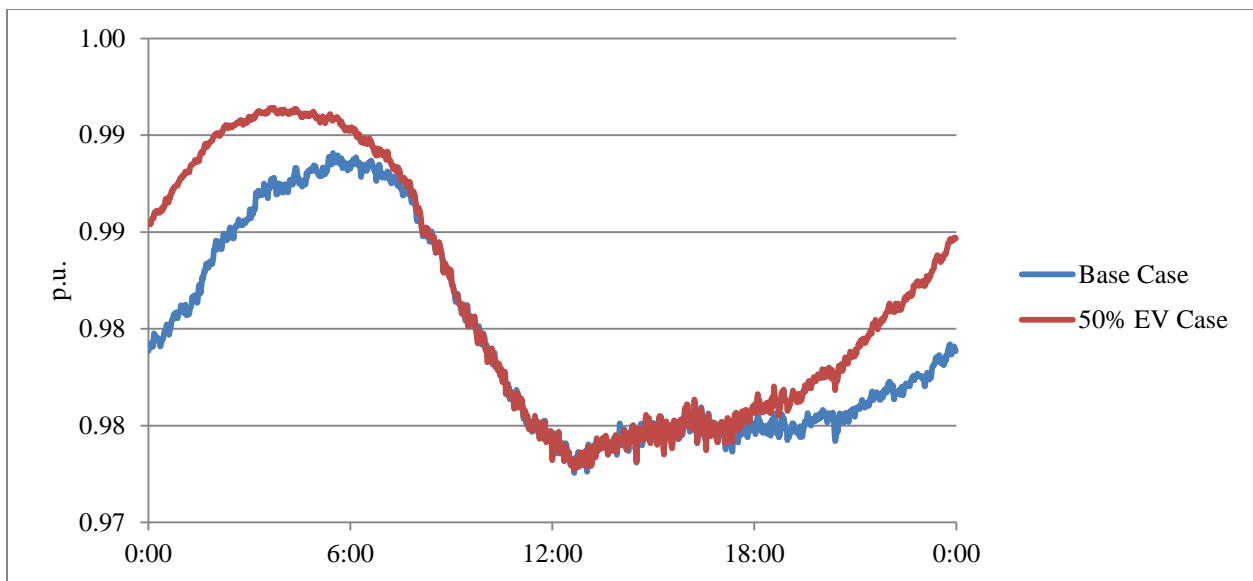


Figure 4.8: Feeder 1515, comparison of base case and 50% EV case, power factor, February 19<sup>th</sup>

Figure 4.8 shows an interesting impact of high penetrations of EVs: there is an improvement in the substation power factor. Commercially-available EV chargers have a near unity power factor, so as more chargers are added to the system, there is an increase in real load with only a negligible increase in reactive load. While the power factor is improved, it should be noted that

it is achieved by further loading the substation with near unity load, which could have other system impacts.

### 4.3 EV Concluding Comments

EVs represent a new end-use load class that have the potential to change the way energy is consumed at the distribution level. Because EVs charge at night time and have no significant day time load, they offer the potential to increase the utilization factor of the distribution system. In reality, end-users often desire to charge their vehicles as soon as they return home from work, which is generally the peak load time. As a result, EVs possess a number of technical challenges that must be addressed before their full benefit can be achieved. This is especially true if utilities desire to use the EVs for other applications such as peak shaving and for providing regulation services.

In the SIS the impact of EVs was examined at two separate levels, the secondary service transformer level and the feeder level. At the service transformer level the possibility of overloading due to coincidental peak loads is the primary concern for EVs. At 50% penetrations this appears to be manageable, but at levels of 100% and 150% the utility would need to install a new service transformer. Reconductoring in addition to a new transformer might be necessary. Penetration levels for a single service transformer should be kept well below 100% unless there is advanced coordination of EV charging that prevents transformer overloads. Another option, possibly much less expensive, is to replace the service transformer with a higher rated unit.

For the feeder level impacts, the primary concern is overloading of the substation transformer. Low feeder penetration levels of 5% are achievable with no changes in the design or operation of the feeder, at 25% penetration peak load increases are seen, and at 50% penetration significant peak load increases are observed. Overloads of the substation transformer(s) are significantly more important than overloads of secondary transformers, because of the size, and cost of and replacement cost of substation transformers. As such, feeder level penetrations of EV should be maintained below 25% unless there is an advanced coordination of EV charging that prevents increases in the feeder peak load.



## 5 MicroDMS Analysis

MicroDMS covers a broad category of management systems that are designed to operate at the sub-feeder level. For the purposes of the SIS, microDMS is a system that operates at the level of the service transformer to reduce the impacts due to PVs and EVs. The SIS will examine four potential microDMS functions. These are not all inclusive, but represent a selection of possible mitigation functions that could be provided by microDMS. The first two microDMS functions will be designed to mitigate the effects of solar transients and the second will be designed to mitigate the effects of EVs.

For this section of the SIS, only feeder 1515 will be examined, since this feeder displayed the most severe reaction to solar transients. The results in this section assume that microDMS is controlling all the units on a system and that there is a 100% participation rate, with the exception of HVAC units that are not able to respond due to operational limitations.

### 5.1 HVAC Load Shedding During Solar Transient

The first microDMS function to be examined is load shedding to offset the voltage drop that is experienced during a cloud transient. The use of load shedding will be examined to reduce the voltage drop shown in Figure 3.12 for feeder 1515. Load shedding will be performed via microDMS which will generate a signal to reduce load during the cloud transient. The HVAC units of the end-use customers and their electric hot water (HW) heaters will be the electrical load responding to the microDMS signal.

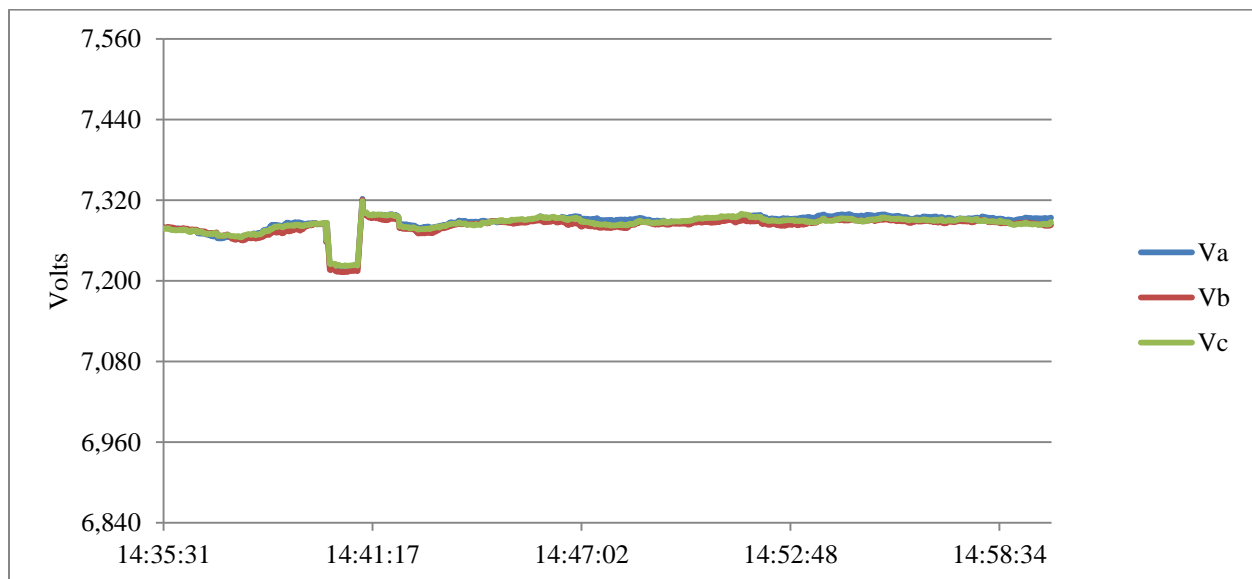


Figure 5.1: Feeder 1515, 50% PV case with 1-minute cloud transient and load shedding, voltages at node N32561, February 19<sup>th</sup> 14:35-15:00

Figure 5.1 shows the time-series voltage on node N32561 during the solar transient when load shedding is initiated by microDMS in an attempt to mitigate the voltage variation caused by the voltage transient. It can be seen that there is still a drop in voltage due to the solar transient, but it is not as extreme as it was in the base case of Figure 3.12. The original voltage drop was approximately 110V and with load shedding this is reduced to approximately 70V. Since the HVAC units and the hot water heating units are the load that is responding to the microDMS signal, we examine their operation in detail. Figure 5.2 and Figure 5.3 show the number of units in operation and the kW demand for the HVAC units and hot water heaters, respectively.

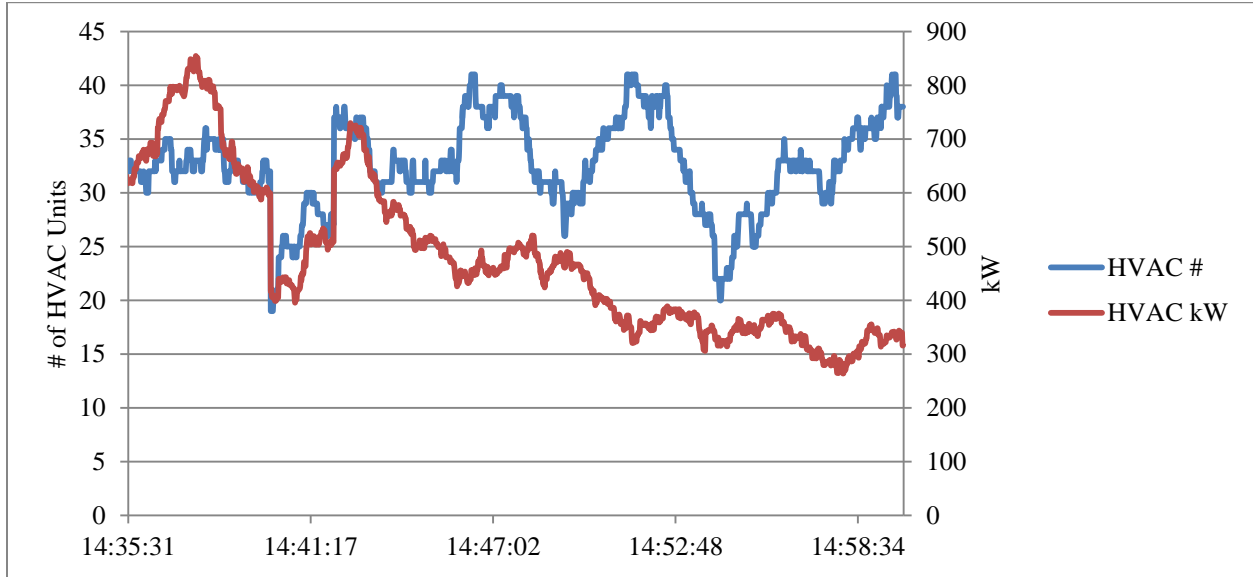


Figure 5.2: Feeder 1515, 50% PV case with 1-minute cloud transient and load shedding, number in operation and total power of HVAC units, February 19<sup>th</sup> 14:35-15:00

From both Figure 5.2 and Figure 5.3, it can be seen that during the cloud transient the number of both HVAC and hot water heaters in operation decreases in response to the microDMS signal. This results in a total load reduction of approximately 500 kW, which is about 20% of the feeder load. Of the 500 kW of load reduction, approximately 40% is supplied by the HVAC units and 60% by the hot water heaters. One key reason for the greater impact from hot water heaters is that when a signal is received, a water heater unit can immediately cut load. In contrast, there are times when it is not desirable for HVAC compressors to be rapidly turned off. Because of the complex refrigeration cycle, damage to a compressor unit can occur if it is short cycled inappropriately.

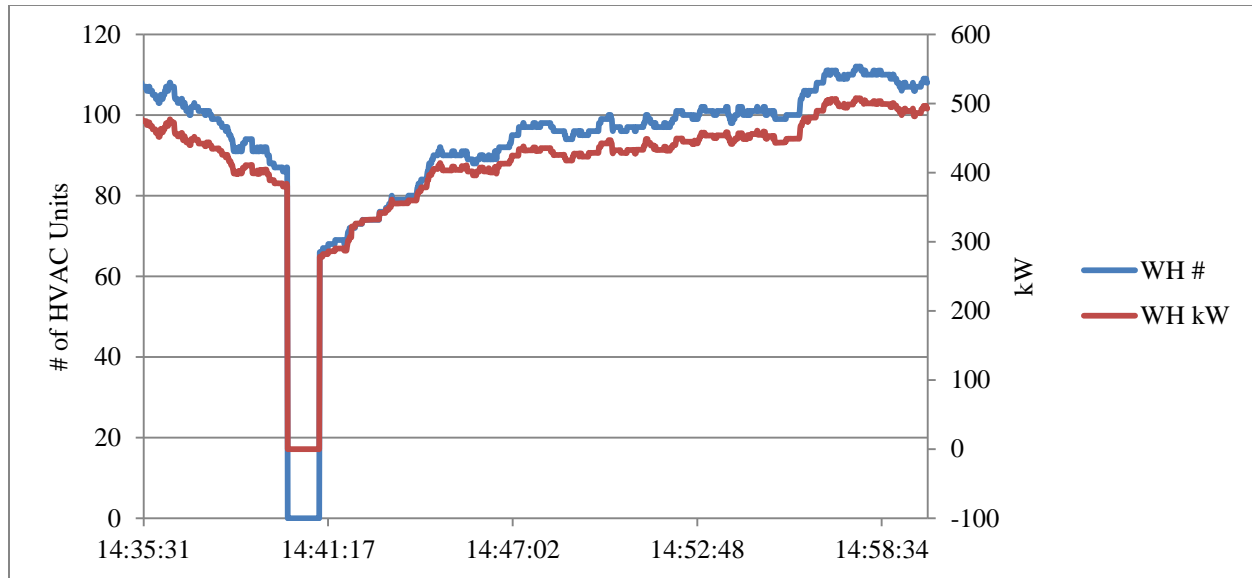


Figure 5.3: Feeder 1515 50% PV case with 1-minute cloud transient and load shedding, number of units in operation and total power of hot water heaters, February 19<sup>th</sup> 14:35-15:00

## 5.2 PV 4-Quadrant Control During Solar Transient

The second microDMS function to be examined is the use of 4-quadrant inverter controls to offset the voltage drop that is experienced during a cloud transient. Under the current IEEE std. 1547, PV inverters are not allowed to perform voltage control, i.e., only real power outputs are allowed. Under normal conditions, the microDMS will signal the PV units to output unity power to achieve the highest financial benefit. But as necessary, the microDMS can coordinate the operation of the inverters in order to adjust the inverter output from real power to reactive power as necessary. Operation in this type of mode, where reactive power can be output, is not in accordance with the current version of IEEE std. 1547, but a soon to be released version of 1547.8 will address this control scheme.

In the first scenario involving 4-quadrant inverter support, the output of the inverters will shift to maximum reactive power output during the cloud transient, while still staying within the kVA rating of the inverters. One issue to note is that PV inverters generally have the capability to provide their rated output in reactive power, even at night time. As a result, with a strong cloud transient where the real power output drops to 20%, the inverter will provide 95% of reactive output without exceeding the apparent power rating. For example, a 5 kVA inverter experiencing a cloud transient will only output 1 kW of real power, which allows up to 4.85 kvar of reactive output while still remaining within the 5 kVA unit rating.

For the 4-quadrant support case, it is assumed that during the cloud transient of Figure 3.12, all of the PV units are coordinated from microDMS units. During the transient the units switch from 100% real power output to maximum available real power output plus maximum reactive

output, up to the kVA rating of the unit. As a result, the PV units go from a unity power factor output to a highly leading power factor. Figure 5.4 shows the voltage at node N32561, the same as Figure 3.12, during the transient.

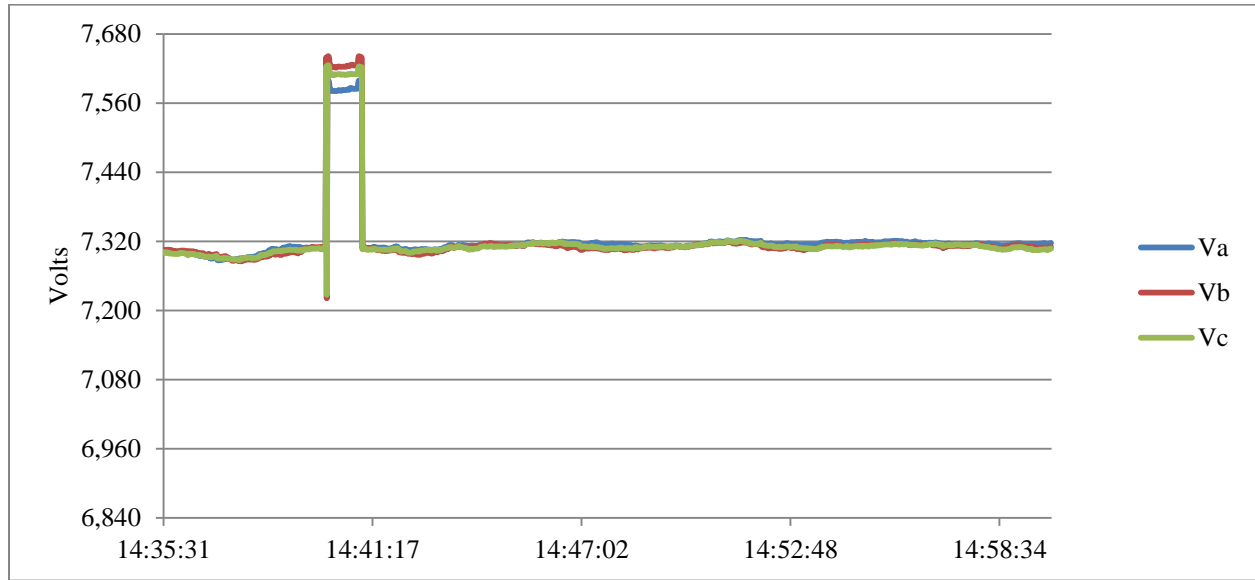


Figure 5.4: Feeder 1515, 50% PV case with 1-minute cloud transient and 100% PV reactive support, voltages at node N32561, February 19<sup>th</sup> 14:35-15:00

In Figure 5.4 it can be seen that there is an initial drop in voltage and then the microDMS begins sending control signals to the PV inverters. The result of the control signals is a large reactive output from all of the inverters. This not only offsets the voltage transient, but it causes a significant over voltage condition which exceeds the ANSI C84.1 high voltage limit. A microDMS system should coordinate the power factor of the PV units to ensure that the low voltage condition is addressed without causing an over-voltage condition.

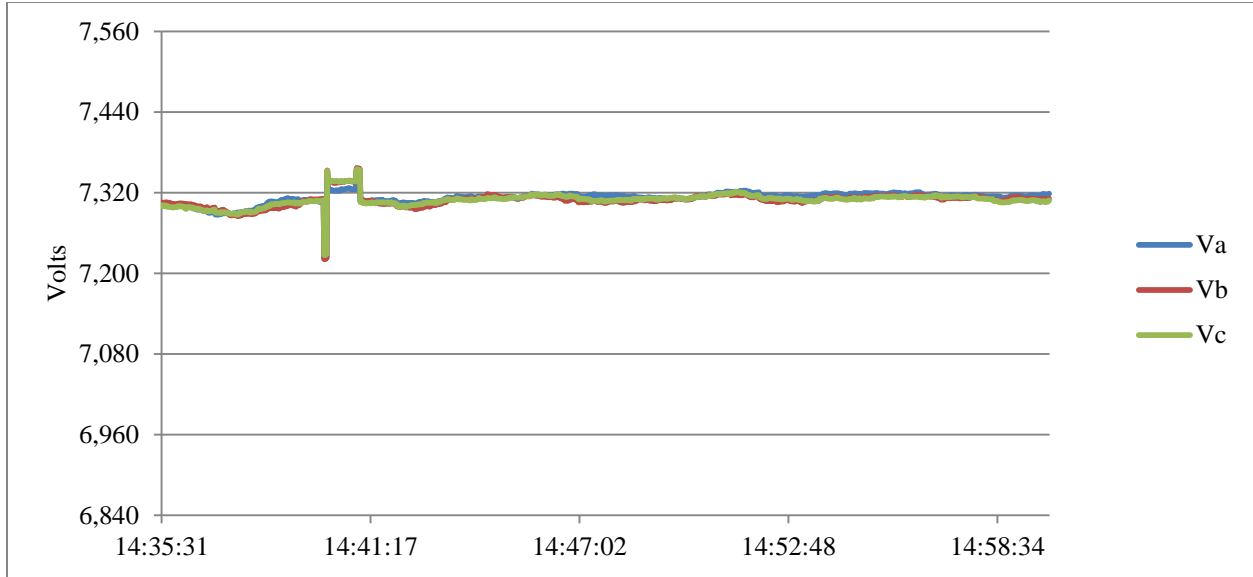


Figure 5.5: Feeder 1515, 50% PV case with 1-minute cloud transient and 30% PV reactive support, voltages at node N32561, February 19<sup>th</sup> 14:35-15:00

Figure 5.5 shows the voltage at node N32561 when the inverters output only 30% of their reactive capability, a leading power factor of 0.56. This achieves the goal of reducing the low voltage condition without a resulting over-voltage condition. The 30% output level for this specific case was not arrived at by an analytic means; it was determined via successive iterations of simulation. A fully functional microDMS needs to be able to determine the proper level of reactive support necessary for a given voltage transient. This could be a difficult challenge with a distributed architecture, so a hierarchical control involving the central DMS could prove beneficial.

### 5.3 Load Shedding to Reduce EV Peak

In contrast to the two previous sections where microDMS was used to address the feeder-level problem of a voltage drop due to a solar transient, this section will examine the use of a microDMS to address overload conditions on a single service transformer. Figure 5.6 shows the loading of the 25 kVA secondary transformer from Figure 4.3, as well as the individual HVAC and HW heating loads. Since it is the HVAC and HW loads that participate in the microDMS control, their contribution to the total load must be examined.

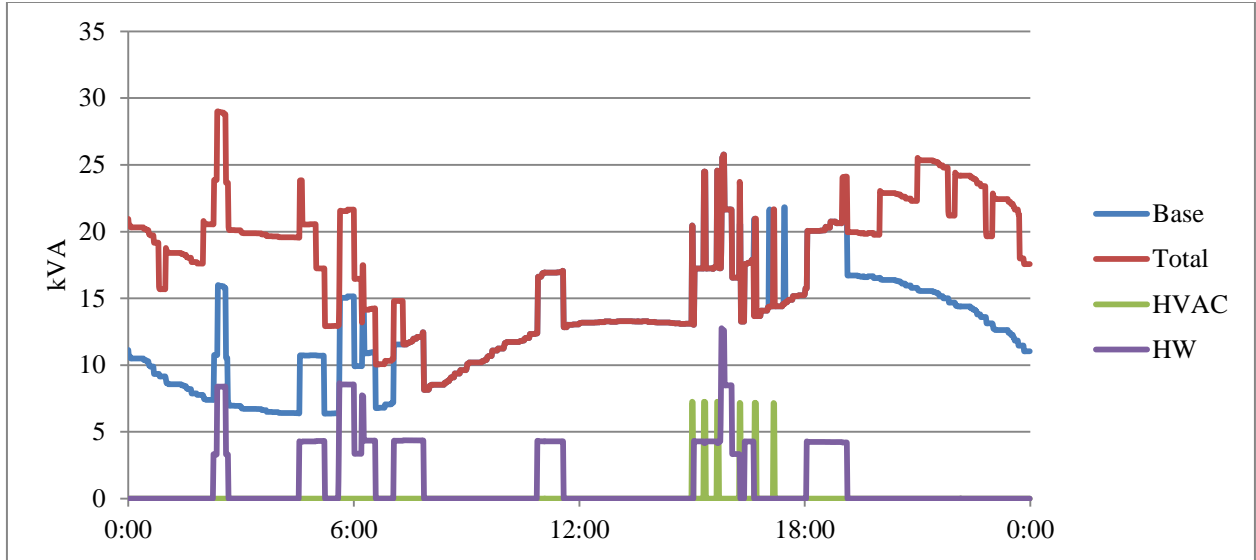


Figure 5.6: 25 kVA transformer, base case and 100% EV case, apparent power loading, with HVAC and hot water heating loads shown separately, February 19<sup>th</sup>

From Figure 5.6, it can be seen that the majority of the HVAC energy consumption occurs during the late afternoon, and contributes to the base case peak load. While shedding HVAC load might be of some use for reducing the base case peak load, it is of no use for reducing the new night time peak load that is caused by EV charging.

HW load occurs at various times throughout the day, including during the new peak load that occurs early in the morning. As a result, a load shedding signal sent to the HW load could make a minor difference. Overall, using load shedding of HVAC and HW loads to offset the overload seen on the secondary service transformer due to EV charging is not practical.

One possible form of load shedding that could be effective, but is not examined in the SIS, is microDMS having control of the EVs that are charging. In this scenario, the microDMS could coordinate the charging of the EVs to reduce transformer overloading due to coincidental peaks.

## 5.4 Battery Operations to Reduce EV Peak

Another possible solution to alleviate overloading of the secondary transformers due to EV charging is the installation of local energy storage that is controlled by the microDMS. While batteries are an expensive solution when compared to installing a larger transformer, they simultaneously perform a number of functions, such as peak reduction, provision of emergency power, and voltage control. For the purposes of the SIS, only the function of peak load reduction will be examined, using a 20 kW, 40 kWh, battery that is connected on the low voltage side of the secondary transformer. While the 20 kW, 40 kWh, battery may be a bit too large for a 25 kVA transformer, it was selected since it is a unit size that will be used in the Japan U.S. Island Grid Project.

Figure 5.7 shows a comparison of the secondary transformer apparent power loading for the 100% EV case and the 100% EV case with a 40 kWh battery. The microDMS is controlling the battery in an attempt to keep the loading below the 25 kVA name plate rating. From Figure 5.7, it can be seen that the microDMS-controlled battery is able to keep the load below the 25 kVA rating of the transformer.

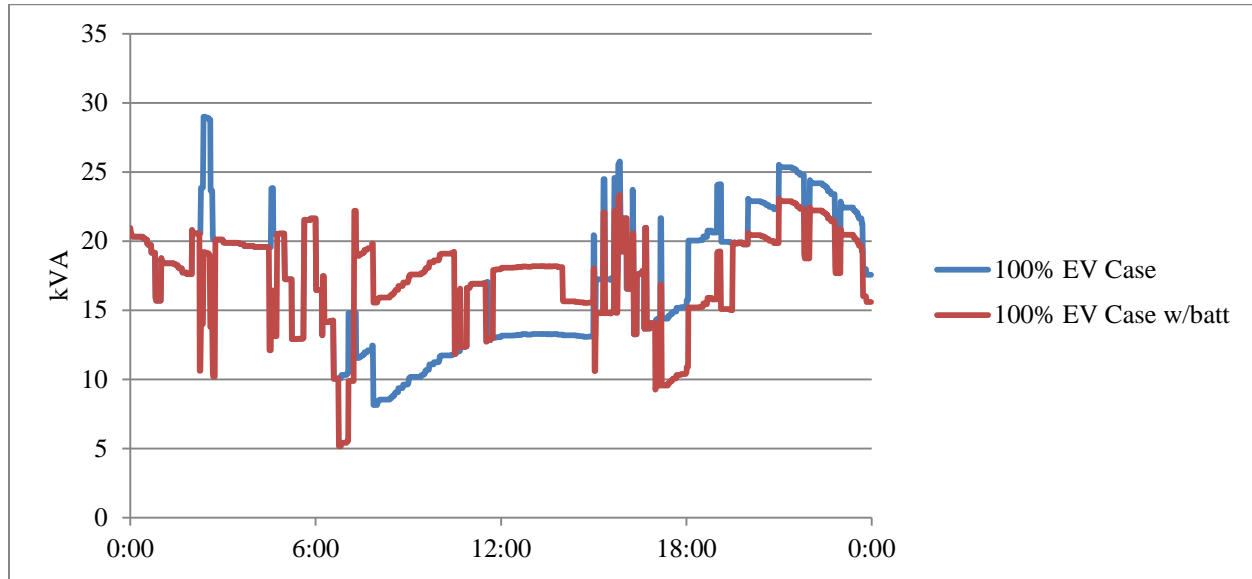


Figure 5.7: 25 kVA transformer, comparison of 100% EV case and 100% EV case with a battery, apparent power, February 19<sup>th</sup>

Figure 5.8 shows the real power output and the State Of Charge (SOC) for the battery over the 24-hour period. It can be seen that the real power output of the battery never exceeds 10 kW, which is only 50% of its rated output. In contrast, nearly the full range of the storage capacity, 40 kWh, is utilized. From this, it can be concluded that for a small 25 kVA transformer, a 20 kW, 40 kWh, battery is more than sufficient to completely offset the overloading conditions that result from charging in the 100% case; 8 EVs.

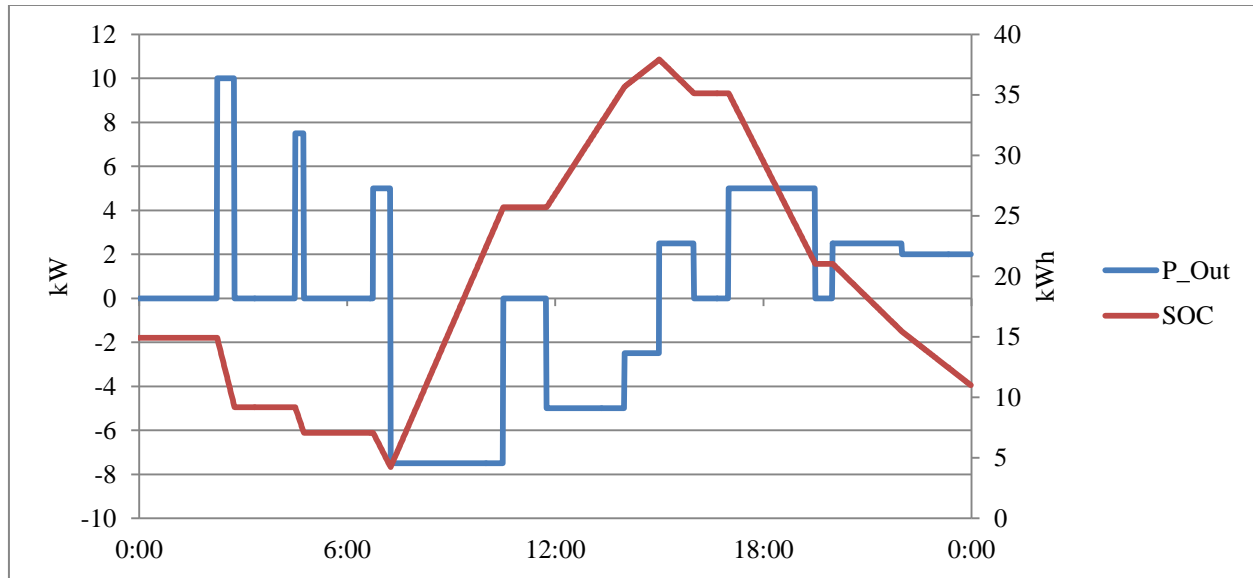


Figure 5.8: 20 kW, 40 kWh, battery power output and state of charge

## 5.5 Micro DMS Concluding Comments

MicroDMS is a concept that encompasses numerous possible capabilities. For the purposes of the SIS microDMS was operated in an effort to offset the negative impacts of PV and EV operations. Specifically, voltage variations on the primary distribution system and overloading of the substation and secondary service transformers were addressed.

MicroDMS was installed at the secondary service transformer, with a coordinating link that ties into the utility's central DMS. This allowed all of the units to coordinate their operations. The microDMS units were able to control the PV inverters as well, as HVAC and hot water heating loads. With these capabilities, four specific applications of microDMS were examined:

- 1) Load shedding during the solar transient: HVAC and hot water heating were interrupted during the transient in an attempt to minimize the magnitude of the voltage drop. This application was only moderately effective since there were a limited number of units in operation during the transient period, and not all of the HVAC units could be interrupted. Additionally, the loads interrupted primarily consumed real power so the effect was less pronounced than if it had included large reactive loads.
- 2) PV 4-quadrant control during solar transient: the inverters were allowed to output reactive power during the transient in an attempt to minimize its magnitude. The magnitude of the reactive power resource was so great that if this was attempted in an uncoordinated manner an over voltage condition would occur, in violation of ANSI C84.1. At the 50% PV case, with all of the inverters participating, a 30% output of reactive power would completely offset the voltage drop due to the solar transient. The use of 4-quadrant PV controls,



assumed to be coordinated by microDMS, proved to be very effective.

- 3) Load shedding to reduce EV peak: the shedding of residential end-use loads was performed in an attempt to reduce the overload condition of the secondary service transformer due to EV charging. HVAC and hot water heating loads were controlled by the microDMS to achieve this goal. Once again, due to the small amount of HVAC and hot water heating on the evening of the 19<sup>th</sup>, significant load reductions may not be consistently achievable.
- 4) Battery operation to reduce EV peak: a 20 kW, 40 kWh, battery at the output of the service transformer was controlled to reduce the overload condition of the secondary service transformer due to EV charging. Unlike load shedding, the battery proved to be highly effective at mitigating overload conditions, including at the 100% penetration level. While the battery was a highly effective solution, it is significantly more costly than a simple replacement of the transformer with a larger unit. With that said, the battery could simultaneously be used for other applications such as islanding, regulation, and voltage control, which were not examined in the SIS.

## 6 System Impact Study Concluding Comments

The system impact study examined the impacts of PVs and EVs on three Kihei distribution feeders, as well as the use of microDMS type technologies to mitigate their impacts. The open source simulation environment GridLAB-D was used to conduct simulation and analysis. The models run in GridLAB-D were obtained from distribution planning models that were modified into time-series models and were calibrated against historic SCADA data. Simulations were run over a three-month period, but February 19<sup>th</sup> was selected for detailed discussion.

The first technology on the Kihei feeders to be examined was distributed solar PV. It was seen that the current penetration of solar PV presented no operational problems, and that the feeders could in fact support a 50% penetration level. Time-series simulations showed that higher levels of PV may cause increased operation of LTCs, but that there would be other significant impacts. The area where high penetration levels of distributed solar PV did pose an issue was during cloud transients. These short duration events, 1-minute or less, occurred so quickly that the LTCs did not have time to respond. As a result, active voltage regulation could not be maintained. Despite this, even at a 50% penetration level, voltages never violated the ANSI C84.1 voltage ranges. In conclusion, the feeders were able to support a 50% penetration level, but higher levels would require the adjustment of existing control devices, or the addition of more voltage control devices.

While distributed PV primarily affected the distribution feeder level voltage, EVs have the greatest impact on the loading of transformers. This is particularly true at the secondary service transformer where lack of load diversity, as well as similarity of socioeconomic conditions, can lead to potentially high penetration levels for a single transformer. For a typical 25 kVA service transformer it was shown that a relatively small number of units could result in an overload condition. Additionally, with as few as 1 EV per house, a transformer could expect to experience sustained overload conditions that impact the effective service life of the unit. In addition to the impacts on individual service transformers, low to moderate penetrations of EV could produce overload conditions on the substation transformer; a significantly larger and more expensive piece of equipment. In conclusion, the feeders are able to support local clusters of EV, with the occasional replacement of service transformers, until the load begins to affect the substation transformer at around 25% penetration. At this penetration level, a coordinated plan would be necessary to effectively operate the feeder without reducing the service life of the transformers.

One potential solution to mitigate the high penetration impacts of distributed PV and EVs is the use of microDMS. MicroDMS refers to a technology with a broad range of capabilities, only a few of which were examined in the SIS. Four specific microDMS functions were examined, with a focus on their ability to mitigate voltage transients due to cloud transients, and to mitigate transformer overloads due to EV charging. The four functions examined were, load shedding to

mitigate the impacts of solar transients, 4-quadrant inverters to mitigate the impact of solar transients, load shedding to mitigate transformer overloading due to EV charging, and the control of batteries to mitigate transformer overloading due to EV charging. In the SIS it was clearly seen that the use of 4-quadrant control on PV inverters was much more effective than load shedding when attempting to mitigate solar transients. Similarly, the control of batteries of was significantly more effective than load shedding to mitigate the overloading of transformers. Overall, microDMS is a promising technology but due to its complexity and cost it should be operated to obtain multiple benefit streams.

This SIS has given an overview of impact of various technologies on three distribution feeders in the MECO service territory. It is not a comprehensive evaluation of all distribution feeders under all conditions. Based on the select results, additional simulation and analysis would be beneficial to MECO and HECO.

## Appendix A: GridLAB-D Simulation Methodology

Simulations of the different project technologies and programs were accomplished using the GridLAB-D software. GridLAB-D provides an agent-based multi-disciplinary environment for the examination and evaluation of emerging technologies. By providing a multi-disciplinary simulation environment, it is possible to bring together diverse teams of experts from multiple fields of study to holistically examine complex systems.

GridLAB-D has been developed through funding from the Department of Energy, Office of Electricity. Through \$5.5 million of direct funding and supporting projects from DOE-OE, GridLAB-D has developed significant capabilities for analyzing smart grid deployments. The capabilities center on the functionality needed to simulate a distribution feeder power flow and attached loads. The development has included: unbalanced three-phase power flow solvers; detailed end-use models, particularly of a residential home's thermal integrity, HVAC cycles and water heater cycles; and a transactive market that supports double auction bidding. Different combinations of these capabilities enabled simulations of the various technologies and programs evaluated in this report.

GridLAB-D conducts time-series simulations with variable time steps. The solution at each time step is a quasi-steady state solution for each of the modules. Convergence is achieved within each module and convergence across modules is coordinated via the GridLAB core as illustrated in Figure A.1.

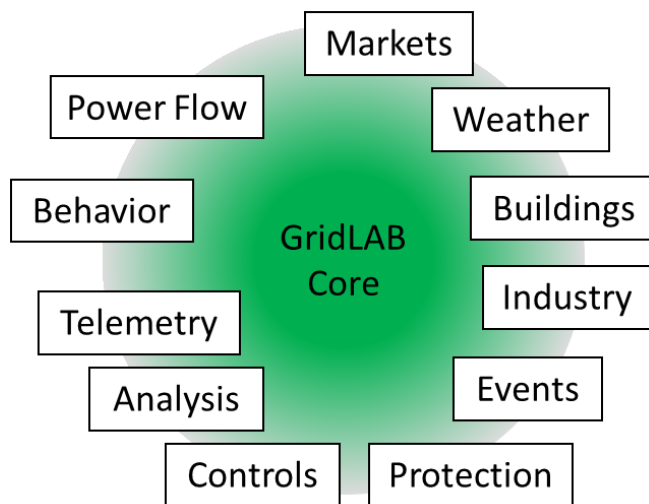


Figure A.1: GridLAB-D architecture

Time steps are also coordinated by the GridLAB-D core. This is necessary because the various modules in the simulation will generally have different time step requirements. At the end of a time step, every object in the model returns a 'sync' time that indicates how long the object will remain constant without outside influence. The GridLAB core then examines every object and

determines what the smallest sync time is; this then becomes length of the next step. This process is performed at every time step so that the system has a variable step size. For a given state variable an example of the variable step sizes are shown in Figure A.2.

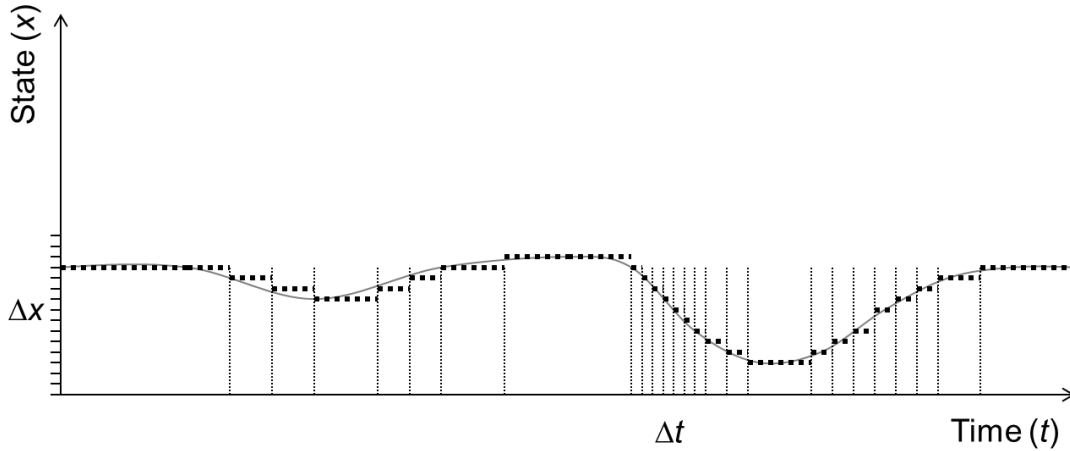


Figure A.2: Variable step sizes in GridLAB-D simulation

When analyzing operations at the distribution level, the major dynamics of interest are mid-term and occur on the order of minutes to hours. For the purposes of this analysis, a minimum time step of one minute was enforced. For operations that occur at intervals of less than one minute, such as a 45-second delay on a voltage regulator, the operation is aggregated up to the one minute time step; multiple operations cannot occur during the enforced minimum of one minute. Because of the large number of objects and the forced minimum, the simulation proceeded at one-minute time steps for the majority of the simulations. As a result, there are approximately 500,000 time steps in an annual simulation of a single prototypical feeder.

Since the simulations for the SIS analysis are being conducted over a 3 month period, the minimum step size has been set to one minute. Even with a minimum one minute step size there is the possibility of 131,250 time steps in a single simulation. For the simulations where one second minimum step size were used simulations were only run for a 24 hours period, but this still resulted in 86,400 time steps in a single simulation.

## References

- [1] <http://sourceforge.net/projects/gridlab-d/>
- [2] American National Standard for Electrical Power Systems and Equipment-Voltage Ratings (60 Hertz), American National Standards Institute C84.1-2006.
- [3] R. S. Briggs, R. G. Lucas, Z. T. Taylor, “Climate Classification for Building Energy Codes and Standards”, ASHRAE Winter Meeting, Chicago, IL, January, 2003
- [4] W. H. Kersting, “Distribution System Modeling and Analysis, 3<sup>rd</sup> Edition”, CRC Press, New York, 2012.
- [5] K. Schneider, J. Fuller, and D. Chassin, “Multi-State Load Models for Distribution System Analysis”, *Accepted IEEE Transactions on Power Systems*.



*Proudly Operated by Battelle Since 1965*

902 Battelle Boulevard  
P.O. Box 999  
Richland, WA 99352  
1-888-375-PNNL (7665)  
[www.pnnl.gov](http://www.pnnl.gov)



U.S. DEPARTMENT OF  
**ENERGY**